mathematics

MDPI

Article

Adaptive Fuzzy Control with Predefined-Time Convergence for High-Order Nonlinear Systems Facing Input Delay and Unmodeled Dynamics

Mohamed Kharrat [1] and Paolo Mercorelli [2,*]

[1] Mathematics Department, College of Science, Jouf University, Sakaka 72388, Saudi Arabia
[2] Institute for Production Technology and Systems, Leuphana University of Lueneburg, 21335 Lueneburg, Germany
* Correspondence: paolo.mercorelli@leuphana.de

Abstract

This work addresses the design of a predefined-time adaptive fuzzy control scheme for high-order nonlinear systems with nonstrict-feedback structures, subject to unmodeled dynamics and input time delay. To mitigate the influence of unmodeled dynamics, a predefined-time auxiliary dynamic signal is incorporated into the controller design. Meanwhile, the adverse effects caused by input delay are handled by integrating a Padé approximation with the introduction of an intermediate state variable. Fuzzy logic systems are utilized to approximate the unknown nonlinear terms present in the system dynamics. Based on a recursive backstepping framework and a power-type Lyapunov function formulation, an adaptive fuzzy tracking controller with predefined-time convergence characteristics is constructed. A detailed stability analysis demonstrates that the closed-loop system achieves practical predefined-time convergence, while appropriate selection of design parameters guarantees that the tracking errors remain confined within a small bounded region around the origin. Finally, the effectiveness and advantages of the proposed control strategy are validated through a numerical example and a practical example.

Keywords: nonlinear systems; adaptive control; predefined-time stability; unmodeled dynamics; input delay

MSC: 93C10; 93C40; 37N35

Academic Editor: Yiu Yin Raymond Lee

Received: 30 January 2026
Revised: 19 February 2026
Accepted: 20 February 2026
Published: 25 February 2026

1. Introduction

The control of high-order nonlinear systems has attracted sustained attention due to their broad applicability in complex engineering processes. Compared with strict-feedback systems, high-order nonlinear systems possess a more general structural form, enabling them to describe complex nonlinear dynamics with higher modeling flexibility. However, this structural generality significantly increases the difficulty of controller design. In particular, conventional feedback linearization techniques may lead to uncontrollable or unobservable modes, which severely restrict their applicability in high-order nonlinear settings [1–3]. To overcome these challenges, a constructive control methodology based on the adding one power integrator technique has been developed, providing a systematic design framework for stabilizing high-order nonlinear systems. This methodology has been extensively extended to adaptive control scenarios to cope with system uncertainties.

In practical applications, many high-order nonlinear systems suffer from modeling inaccuracies and external disturbances. The assumption of precisely known nonlinear dynamics is often unrealistic, which limits the effectiveness of classical control approaches. To address this issue, intelligent adaptive control strategies employing fuzzy logic systems and neural networks have been introduced. Due to their strong approximation and learning capabilities, these approaches can perform online estimation of unknown nonlinear functions, allowing for enhanced robustness and tracking performance [4,5]. Various adaptive control strategies have been proposed in the literature; for instance, adaptive control for high-order nonlinear multi-agent systems under event-triggered communication protocols has been investigated to reduce communication load while maintaining coordinated tracking accuracy [6]. An adaptive dynamic surface control scheme incorporating parameter estimation has also been developed to alleviate the computational complexity of backstepping in strict-feedback systems [7]. Moreover, adaptive neural control frameworks with dynamic memory and event-triggered mechanisms have been introduced for stochastic nonlinear systems subject to delayed output constraints [8]. Adaptive tracking control approaches for nonlinear systems with time-varying delays and asymmetric output constraints have been reported as well [9].

Despite these developments, unmodeled dynamics remain a fundamental challenge in practical control systems. Unmodeled dynamics may arise from neglected high-order system behaviors, actuator dynamics, or unknown nonlinear effects that are not explicitly included in the nominal model [10–12]. Their presence can degrade tracking accuracy, slow down transient response, and even cause instability [13]. Consequently, significant research efforts have focused on designing adaptive control schemes capable of compensating for unmodeled dynamics while preserving stability and satisfactory performance [14–16]. For example, adaptive control methods have been proposed for nonlinear systems with input delays, unknown dead-zone nonlinearities, and unmodeled dynamics [17]. Neural network–based adaptive control has been developed for fractional-order systems with actuator faults and unmodeled uncertainties [18]. Event-triggered fuzzy adaptive finite-time control has been investigated for stochastic nonlinear systems with unmodeled dynamics [19]. Furthermore, adaptive control approaches for pure-feedback nonlinear systems under time-varying state constraints and unmodeled dynamics have been proposed to guarantee closed-loop stability [20].

Another practical factor that significantly affects system performance is input delay. Input delay commonly arises from actuator dynamics, signal transmission processes, communication constraints, and hardware limitations [21]. If not properly addressed, input delay may deteriorate transient response, reduce tracking precision, and even destabilize the closed-loop system. Various strategies based on compensation or approximation have been proposed to mitigate delay effects [22,23]. Among these, the Padé approximation method has been widely adopted due to its ability to convert the delayed input into an equivalent delay-free representation, allowing for simplified controller design. Several adaptive control schemes incorporating delay compensation have been developed in different contexts [24–26]. For instance, finite-time adaptive prescribed performance control has been proposed for nonlinear systems with input delay [27]. Adaptive tracking control based on multi-dimensional Taylor network approximations has been reported to enhance robustness against delay and dynamic uncertainties [28]. Reinforcement learning-based adaptive backstepping control for nonlinear systems with input delay has been explored as well [29]. In addition, adaptive neural control for nonstrict-feedback stochastic nonlinear systems with input delay has been investigated as a way to guarantee stability under randomness and delayed control actions [30].

In addition to uncertainty and delay issues, convergence performance has become an increasingly important design objective. Although finite-time control ensures convergence within a finite duration, the settling time generally depends on initial conditions. Fixed-time control eliminates this dependence and guarantees convergence within a bounded time independent of initial states [31,32]. Nevertheless, the convergence bound in fixed-time control often depends on multiple design parameters and may be conservative in practice [33–35]. In applications requiring strict time performance guarantees, such as aircraft attitude control, multi-agent coordination, and cooperative robotic systems, convergence within a precisely specified time interval is essential. To address this requirement, predefined-time control has been introduced, where the settling time is explicitly determined by a user-selected parameter rather than the initial condition [36–38]. This property allows the convergence time to be assigned a priori according to performance specifications. Recent studies have developed adaptive predefined-time control frameworks for various nonlinear systems [39–42]. Representative works include predefined-time adaptive fuzzy control for systems with input saturation and delayed constraints [43], adaptive predefined-time control for stochastic switched nonlinear systems with quantization [44], adaptive fuzzy predefined-time fault-tolerant control [45], and predefined-time tracking control for nonstrict-feedback high-order nonlinear systems with input quantization [46].

Although considerable progress has been achieved, several limitations remain. Existing studies typically focus separately on either input delay compensation, unmodeled dynamics handling, or predefined-time convergence. The integrated treatment of high-order nonstrict-feedback nonlinear systems that simultaneously involve unmodeled dynamics, input delay, and predefined-time stability guarantees remains relatively underexplored. Moreover, combining intelligent adaptive fuzzy approximation mechanisms with rigorous predefined-time stability analysis under such complex structural conditions presents significant theoretical and practical challenges. Motivated by these observations, this paper develops a predefined-time adaptive fuzzy control framework for high-order nonstrict-feedback nonlinear systems with unmodeled dynamics and input delay. The proposed method aims to achieve accurate tracking within a designer-assigned time while ensuring robustness against dynamic uncertainties and delay effects. By integrating fuzzy approximation techniques with predefined-time stability theory and delay compensation via Padé approximation, the proposed approach provides both rigorous theoretical guarantees and practical applicability for complex nonlinear systems. Based on the above analysis, the main contributions of this work are summarized as follows:

(i) A predefined-time adaptive fuzzy control scheme is proposed for high-order nonstrict-feedback nonlinear systems in the presence of unmodeled dynamics and input delay. Compared with the finite-time and fixed-time control approaches reported in [30–35], the proposed method guarantees convergence within a designer-assigned time horizon determined explicitly by a tunable parameter. The Padé approximation technique is incorporated to compensate for input delay, ensuring closed-loop stability and satisfactory tracking performance.

(ii) A dynamic predefined-time control structure is constructed to handle unmodeled dynamics and actuator nonlinearities. The proposed scheme guarantees practical predefined-time stability, meaning that system states converge to a small neighborhood around the origin within the prescribed time. Through appropriate parameter selection, tracking accuracy can be improved while maintaining robustness against modeling uncertainties and external disturbances.

The remainder of this paper is organized as follows: Section 2 presents the problem formulation along with the required preliminary concepts; the design of the adaptive tracking controller and the associated stability analysis are detailed in Section 3; simulation

results and a representative practical application are provided in Section 4 to demonstrate the performance of the proposed method; finally, Section 5 concludes the paper and outlines potential directions for future investigation.

2. Problem Formulation and Preliminaries

Consider a class of high-order nonlinear systems with a nonstrict-feedback structure, which can be expressed as

$$\begin{cases} \dot{\xi} = q(\xi, x), \\ \dot{x}_\iota = x_{\iota+1}^{\sigma_\iota} + f_\iota(x) + \Delta_\iota(x, \xi, t), \quad \iota = 1, 2, \ldots, h-1, \\ \dot{x}_h = u^{\sigma_h}(t-\tau) + f_h(x) + \Delta_h(x, \xi, t), \\ y = x_1. \end{cases} \tag{1}$$

Here, the system state vector is defined as $x = x_h = [x_1, \ldots, x_h]^T \in \mathbb{R}^h$, with the partial state vector $x_\iota = [x_1, \ldots, x_\iota]^T \in \mathbb{R}^\iota$. The constants $\sigma_\iota \geq 1$ are odd integers, the functions $f_\iota(x)$ denote unknown smooth nonlinearities satisfying $f_\iota(0) = 0$, and the variable ξ represents unmeasured internal state dynamics, where the ξ-subsystem corresponds to unmodeled dynamics. The terms $\Delta_\iota(\cdot)$ describe unknown nonlinear disturbances acting on the system. It is assumed that $q(\cdot)$ and $\Delta_\iota(\cdot)$ are uncertain but locally Lipschitz-continuous. The scalar variables $u \in \mathbb{R}$ and $y \in \mathbb{R}$ denote the control input and system output, respectively. Finally, τ represents an unknown input delay, which is assumed to be a positive constant.

To address the input delay appearing in the high-order nonlinear system in (1), the Padé approximation technique is employed following the approach in [21]. By virtue of the delay property of the Laplace transform, the following relationship holds:

$$\mathcal{L}\{u^{\sigma_h}(t-\tau)\} = e^{-\tau v}\mathcal{L}\{u^{\sigma_h}(t)\} = \frac{exp(-\tau v/2)}{exp(\tau v/2)} \tag{2}$$

where v denotes the Laplace variable. Using the first-order Padé approximation, one has

$$exp(-\tau v)\mathcal{L}\{u^{\sigma_h}(t)\} \approx \frac{1-\frac{\tau v}{2}}{1+\frac{\tau v}{2}}\mathcal{L}\{u^{\sigma_h}(t)\}, \tag{3}$$

where $\mathcal{L}\{u(t)\}$ is the Laplace transform of $u(t)$.

Remark 1. *Due to the inherent limitation of the Padé approximation, the proposed approach is applicable to systems with small input delays. When τ is sufficiently small, the approximation error $e^{-\tau v} - \frac{1-\frac{\tau v}{2}}{1+\frac{\tau v}{2}}$ is negligible. Extension to large or time-varying delays will be investigated in future work.*

To facilitate controller design, an auxiliary state x_{h+1} is introduced such that

$$\frac{1-\frac{\tau v}{2}}{1+\frac{\tau v}{2}}\mathcal{L}\{u^{\sigma_h}(t)\} = \mathcal{L}\{x_{h+1}(t)\} - \mathcal{L}\{u^{\sigma_h}(t)\}. \tag{4}$$

Rearranging the above equation yields

$$2\mathcal{L}\{u^{\sigma_h}(t)\} = \mathcal{L}\{x_{h+1}(t)\} + \frac{\tau v}{2}\mathcal{L}\{x_{h+1}(t)\}. \tag{5}$$

Applying the inverse Laplace transform gives

$$\dot{x}_{h+1} = \frac{4}{\tau}u^{\sigma_h} - \frac{2}{\tau}x_{h+1}. \tag{6}$$

Defining $\lambda = 2/\tau$, *the above equation can be rewritten as*

$$\dot{x}_{h+1} = 2\lambda u^{\sigma_h} - \lambda x_{h+1}. \tag{7}$$

Following the aforementioned transformations, the delayed system in (1) can be reformulated into an equivalent delay-free augmented representation, provided by

$$\begin{cases} \dot{\xi} = q(\xi, x), \\ \dot{x}_\iota = x_{\iota+1}^{\sigma_\iota} + f_\iota(x) + \Delta_\iota(x, \xi, t), \quad \iota = 1, \ldots, h-1, \\ \dot{x}_h = x_{h+1} - u^{\sigma_h} + f_h(x) + \Delta_h(x, \xi, t), \\ \dot{x}_{h+1} = -\lambda x_{h+1} + 2\lambda u^{\sigma_h}, \\ y = x_1. \end{cases} \tag{8}$$

The objective of this study is to develop a predefined-time adaptive control strategy based on fuzzy logic systems for the system in (1) such that all closed-loop signals remain bounded within a designer-specified time interval and the output tracking error converges to a sufficiently small neighborhood of the origin.

Assumption 1 ([13]). *For each* $\iota = 1, 2, \ldots, h$, $\exists$ *known, smooth, and non-negative functions* $\Psi_{\iota,1}(\cdot)$ *and* $\Psi_{\iota,2}(\cdot)$ *satisfying*

$$|\Delta_\iota(x, \xi, t)| \leq \Psi_{\iota,1}(|x_\iota|) + \Psi_{\iota,2}(|\xi|). \tag{9}$$

Moreover, without imposing any restriction on generality, the function $\Psi_{\iota,2}(\cdot)$ *is assumed to satisfy* $\Psi_{\iota,2}(0) = 0$.

Assumption 2 ([19]). *Consider the* ξ*-subsystem* $\dot{\xi} = q(\xi, x)$ *associated with system (1). There exist class* $\mathcal{K}_\infty$ *functions* $\underline{\mathcal{L}}(\cdot)$, $\overline{\mathcal{L}}(\cdot)$, *and* $\eta(\cdot)$ *together with positive constants* a *and* ω *such that an exponentially input-to-state practically stable (Exp-ISpS) Lyapunov function* $V(\xi)$ *can be constructed satisfying*

$$\underline{\mathcal{L}}(\xi) \leq V(\xi) \leq \overline{\mathcal{L}}(\xi) \tag{10}$$

and

$$\frac{\partial V(\xi)}{\partial \xi} q(\xi, x) \leq -aV(\xi) + \eta(|x_1|) + \omega. \tag{11}$$

Assumption 3 ([47]). *Define* σ_ι *for* $\iota = 1, 2, \ldots, h$ *as positive odd integers and let* $\sigma = \max_{\iota=1,2,\ldots,h}\{\sigma_\iota\}$. *The odd integers* σ_ι *satisfy the inequality*

$$\frac{\sigma + 1}{\sigma_\iota} \geq \sigma - \sigma_{\iota+1} + 1, \quad \iota = 1, 2, \ldots, h-1. \tag{12}$$

Assumption 4 ([35]). *The reference trajectory* $y_r(t)$ *together with its derivative of order* h *is assumed to be smooth and uniformly bounded for all time.*

Lemma 1 ([48]). *Given arbitrary real scalars* $\mathcal{P}$ *and* $\mathcal{N}$ *along with any prescribed positive constants* $\tilde{c}$, $\tilde{d}$, *and* ε, *the following result holds:*

$$|\mathcal{P}|^{\tilde{c}}|\mathcal{N}|^{\tilde{d}} \leq \frac{\tilde{c}}{\tilde{c}+\tilde{d}}\varepsilon|\mathcal{P}|^{\tilde{c}+\tilde{d}} + \frac{\tilde{d}}{\tilde{c}+\tilde{d}}\varepsilon^{-\frac{\tilde{c}}{\tilde{d}}}|\mathcal{N}|^{\tilde{c}+\tilde{d}}. \tag{13}$$

Lemma 2 ([38]). *Assume that conditions (10) and (11) are satisfied. Under these conditions, the function* $V(\xi)$ *qualifies as an exponentially input-to-state practically stable (Exp-ISpS) Lyapunov function for the subsystem* $\dot{\xi} = q(\xi, x)$. *Let* g_0^- *and* g_0^+ *be positive constants satisfying*

$g_0^- = \left(\frac{3}{\delta_0}\right)^{\frac{\zeta}{2}} \frac{\pi}{\zeta T_d}$, $g_0^+ = \frac{j_0^{\frac{\zeta}{2}}\pi}{\frac{\pi}{\zeta T_d}}$ *and define* $g_0 = g_0^- + g_0^+ \in (0, g)$. *For any initial time* $t_0 \geq 0$ *and initial condition* $\xi(t_0) = \tau_0$ *and for any continuous function* $\bar{\eta}(\cdot)$ *satisfying* $\bar{\eta}(x_1) \geq \eta(|x_1|)$, *there exists a predefined time* $T_0 = T_0(g_0^-, g_0^+, r_0, \tau_0) \geq 0$, *a positive constant* $\omega = \bar{\omega} + g_0^+ \frac{\zeta}{2}\left(\frac{2}{2-\zeta}\right)^{\frac{\zeta-2}{\zeta}}$, *and a non-negative function* $B(t_0, t)$ *defined for all* $t \geq t_0$ *such that the auxiliary signal* $r(t)$ *satisfies*

$$\dot{r} = -g_0^- r^{1+\frac{\zeta}{2}} - g_0^+ r^{1-\frac{\zeta}{2}} + \bar{\eta}(x_1) + \bar{\omega}, \quad r(t_0) = r_0. \tag{14}$$

Moreover, the function $B(t_0, t)$ *satisfies* $B(t_0, t) = 0, \quad \forall\, t \geq t_0 + T_0$ *and the Lyapunov function is bounded by*

$$V(\xi(t)) \leq r(t) + B(t_0, t). \tag{15}$$

The solution of the system exists for all $t \geq t_0$. *Without loss of generality, the function* $\bar{\eta}(x_1)$ *is chosen as* $\bar{\eta}(x_1) = x_1^2 \lambda(x_1^2)$, *under which the auxiliary dynamic signal can be rewritten as*

$$\dot{r} = -g_0^- r^{1+\frac{\zeta}{2}} - g_0^+ r^{1-\frac{\zeta}{2}} + x_1^2 \lambda(x_1^2) + \bar{\omega}, \quad r(t_0) = r_0, \tag{16}$$

where $\lambda(\cdot)$ *denotes a smooth non-negative function.*

Lemma 3 ([38]). *For arbitrary real-valued functions* $\mathcal{J}_1$ *and* $\mathcal{J}_2$, *any odd integer* $\sigma > 1$, *and a given constant* $k > 0$, *one has*

$$\left|\mathcal{J}_1^\sigma - \mathcal{J}_2^\sigma\right| \leq \sigma \left|\mathcal{J}_1 - \mathcal{J}_2\right| \left(\mathcal{J}_1^{\sigma-1} + \mathcal{J}_2^{\sigma-1}\right), \tag{17}$$

$$\left|\mathcal{J}_1 + \mathcal{J}_2\right|^k \leq c_k \left(\left|\mathcal{J}_1\right|^k + \left|\mathcal{J}_2\right|^k\right), \tag{18}$$

where $c_k = 1$ *for* $k < 1$ *and* $c_k = 2^{k-1}$ *for* $k \geq 1$. *In this work, the exponent is selected as* $k = \sigma_\iota - 1$. *For notational convenience, both cases are unified as*

$$\left\|\mathcal{J}_1 + \mathcal{J}_2\right\|^k \leq 2^k \left(\left|\mathcal{J}_1\right|^k + \left|\mathcal{J}_2\right|^k\right). \tag{19}$$

Lemma 4 ([49]). *Let* $\varpi > 1$ *and* $\mu > 0$ *be constants and define the set* $\Omega_\chi = \{\chi \in \mathbb{R} \,|\, |\chi| < \varrho\mu\}$, $\varrho = \operatorname{arctanh}\left(\varpi\sqrt{\frac{1}{\varpi}}\right)$. *Then, for all* $\chi \notin \Omega_\chi$, *the inequality* $1 - \varpi \tanh^\varpi\left(\frac{\chi}{\mu}\right) \leq 0$ *is satisfied.*

Lemma 5 ([38]). *For any* $\chi \in \mathbb{R}$ *and any constant* $l > 0$, *the following inequality holds:* $0 \leq |\chi| - \chi \tanh\left(\frac{\chi}{l}\right) \leq p_0 l, \quad p_0 = 0.2785$.

Lemma 6 ([38]). *Let* $f(\chi)$ *be an unknown continuous function defined on a compact set* Ω. *For any prescribed constant* $\varepsilon > 0$, *there exists a fuzzy logic system (FLS) of the form* $W^T\Phi(\chi)$ *such that*

$$\sup_{\chi \in \Omega} \left|f(\chi) - W^T\Phi(\chi)\right| \leq \varepsilon, \tag{20}$$

where $W = [W_1, W_2, \ldots, W_M]^T$ *denotes the adjustable weight vector,* ε *represents the minimum approximation error, and* $M > 1$ *is the number of fuzzy inference rules. The fuzzy basis function vector is defined as* $\Phi(\chi) = \frac{[\Phi_1(\chi), \Phi_2(\chi), \ldots, \Phi_M(\chi)]^T}{\sum_{L=1}^M \Phi_L(\chi)}$, *where each basis function* $\Phi_L(\chi)$ *is selected as a Gaussian membership function given by*

$$\Phi_L(\chi) = \exp\left[-\frac{(\chi - \mu_L)^T(\chi - \mu_L)}{G_L^2}\right], \quad L = 1, 2, \ldots, M, \tag{21}$$

with μ_L *and* G_L *denoting the center and width parameters of the Gaussian function, respectively.*

Lemma 7 ([38]). *Let* $Z = [z_1, z_2, \ldots, z_h]^T$ *be the input vector and let* $\Phi(Z) = [\Phi_1(Z), \Phi_2(Z), \ldots, \Phi_l(Z)]^T$ *denote the corresponding fuzzy basis function vector. For any positive integer* $\iota \leq h$, *define* $\Xi_\iota = [z_1, z_2, \ldots, z_\iota]^T$. *Then, the following inequality holds:*

$$\|\Phi(Z)\|^2 \leq \|\Phi(\Xi_\iota)\|^2. \tag{22}$$

Consider the nonlinear dynamical system

$$\dot{\chi} = f(\chi), \tag{23}$$

where $\chi \in \mathbb{R}^h$ *denotes the state vector, the origin* $\chi = 0$ *is an equilibrium point, and* $f : \mathbb{R}^h \to \mathbb{R}^h$ *is a nonlinear mapping.*

Definition 1 ([38]). *Let* $T_d > 0$ *and* $X > 0$ *be given constants. If the state trajectory o satisfies* $\|\chi(t)\| < X$ *for all* $t > T_d$, *then the equilibrium point at the origin is said to be practically predefined-time stable. The constant* T_d *is referred to as the predefined time.*

Lemma 8 ([38]). *Assume that there exists a Lyapunov function* $V(\chi)$ *such that*

$$\dot{V} \leq -\frac{\pi}{\zeta T_d} V^{1+\frac{\zeta}{2}} - \frac{\pi}{\zeta T_d} V^{1-\frac{\zeta}{2}} + B, \tag{24}$$

where $0 < \zeta < 1$ *and where* T_d *and* B *are strictly positive constants. Under these conditions, the function* V *guarantees practical predefined-time stability, and the corresponding settling time is bounded above by* $2T_d$.

3. Controller Design and Stability Analysis

To facilitate the construction of the desired control law, the following error coordinate transformations are introduced:

$$\begin{cases} z_1 = x_1 - y_r, \\ z_\iota = x_\iota - \alpha_{\iota-1}, \quad \iota = 2, 3, \ldots, h-1, \\ z_n = x_n - \alpha_{h-1} + x_{h+1}/\lambda, \end{cases} \tag{25}$$

where $\alpha_{\iota-1}$ denotes the virtual control signal to be designed subsequently.

Step 1: From (1) and (25), the time derivative of z_1 is obtained as

$$\dot{z}_1 = x_2^{\sigma_1} + f_1(x) + \Delta_1(x, \xi, t) - \dot{y}_r. \tag{26}$$

To analyze the stability of the first subsystem, consider the following power-type Lyapunov function:

$$V_1 = \frac{z_1^{\sigma-\sigma_1+2}}{\sigma-\sigma_1+2} + \frac{\tilde{\Theta}_1^2}{2\tau_1} + r^{\delta_0} \tag{27}$$

where $\hat{\Theta}_1$ is the estimate of the unknown parameter Θ_1^* and $\tilde{\Theta}_1 = \Theta_1^* - \hat{\Theta}_1$ denotes the corresponding estimation error. The design parameters τ_1 and δ_0 are chosen as positive constants. By invoking Assumption 1 together with (16), the time derivative of the Lyapunov function V_1 satisfies

$$\begin{aligned}\dot{V}_1 \le\ & z_1^{\sigma-\sigma_1+1}\left(x_2^{\sigma_1}+f_1(x)-\dot{y}_r\right)+z_1^{\sigma-\sigma_1+1}\Psi_{1,1}(|x_1|)\\ & +z_1^{\sigma-\sigma_1+1}\Psi_{1,2}(|\xi|)-\frac{1}{\tau_1}\tilde{\Theta}_1\dot{\hat{\Theta}}_1-\frac{g_0^-}{\delta_0}r^{1+\frac{\zeta}{2}}-\frac{g_0^+}{\delta_0}r^{1-\frac{\zeta}{2}}\\ & +\frac{1}{\delta_0}x_1^2\lambda(x_1^2)+\frac{\bar{\omega}}{\delta_0}.\end{aligned} \tag{28}$$

Applying Lemma 5, the term $z_1^{\sigma-\sigma_1+1}\Psi_{1,1}(\|x_1\|)$ can be upper-bounded as

$$z_1^{\sigma-\sigma_1+1}\Psi_{1,1}(|x_1|)\le z_1^{\sigma-\sigma_1+1}\hat{\Psi}_{1,1}(x_1)+l_{1,1}^*, \tag{29}$$

where $l_{1,1}>0$ is a design constant, $\hat{\Psi}_{1,1}(x_1)=\Psi_{1,1}(|x_1|)\tanh\left(\frac{z_1^{\sigma-\sigma_1+1}\Psi_{1,1}(\|x_1\|)}{l_{1,1}}\right)$, and $l_{1,1}^*=0.2785\,l_{1,1}$.

Utilizing Assumption 2 together with Lemmas 2 and 5, and following estimation techniques similar to those developed in [25], the following upper bound can be derived:

$$z_1^{\sigma-\sigma_1+1}\Psi_{1,2}(|\xi|)\le z_1^{\sigma-\sigma_1+1}\hat{\Psi}_{1,2}(x_1,r)+l_{1,2}^*+\frac{1}{4}z_1^{2(\sigma-\sigma_1+1)}+m_1(t_0,t) \tag{30}$$

where $l_{1,2}>0$ is a design parameter and $\mathcal{L}^{-1}(\cdot)$ denotes the inverse of the $\mathcal{L}(\cdot)$ function introduced in Assumption 2. The estimated function $\hat{\Psi}_{1,2}(x_1,r)$ is defined as $\hat{\Psi}_{1,2}(x_1,r)=\left(\Psi_{1,2}\circ\mathcal{L}^{-1}\right)(2r)\tanh\left(\frac{z_1^{\sigma-\sigma_1+1}\left(\Psi_{1,2}\circ\mathcal{L}^{-1}\right)(2r)}{l_{1,2}}\right)$, with $l_{1,2}^*=0.2785\,l_{1,2}$. Moreover, the composite function $\left(\Psi_{1,2}\circ\mathcal{L}^{-1}\right)\left(r(t)+B(t_0,t)\right)=\Psi_{1,2}\left[\mathcal{L}^{-1}\left(r(t)+B(t_0,t)\right)\right]$ and $m_1(t_0,t)=\left(\left(\Psi_{1,2}\circ\mathcal{L}^{-1}\right)\left(2M(t_0,t)\right)\right)^2$, where $m_1(t_0,t)\ge 0$ for all $t\ge t_0+T_0$.

Remark 2. *It is worth noting that the term* $\frac{x_1^2\lambda(x_1^2)}{\delta_0 z_1^{\sigma-\sigma_1+1}}$ *is discontinuous at* $z_1=0$*, which prevents its direct approximation using fuzzy logic systems. To overcome this difficulty, a smooth hyperbolic tangent function* $\tanh^{\sigma-\sigma_1+2}\left(\frac{z_1}{\mu}\right)$ *with a given constant* $\mu>0$ *is introduced. As a result, the expression* $z_1^{\sigma-\sigma_1+2}\tanh^{\sigma-\sigma_1+2}\left(\frac{z_1}{\mu}\right)$ *becomes well defined and continuous at* $z_1=0$*.*

Using (29) and (30) in (28), one has

$$\begin{aligned}\dot{V}_1 \le\ & z_1^{\sigma-\sigma_1+1}\left(x_2^{\sigma_1}+\bar{f}_1(x)-\dot{y}_r\right)-\frac{1}{2}z_1^{2(\sigma-\sigma_1+1)}-\frac{1}{\tau_1}\tilde{\Theta}_1\dot{\hat{\Theta}}_1\\ & -\frac{g_0^-}{\delta_0}r^{1+\frac{\zeta}{2}}-\frac{g_0^+}{\delta_0}r^{1-\frac{\zeta}{2}}+\left(1-(\sigma-\sigma_1+2)\tanh^{\sigma-\sigma_1+2}\left(\frac{z_1}{\mu}\right)\right)\frac{x_1^2\lambda(x_1^2)}{\delta_0}\\ & +l_{1,1}^*+l_{1,2}^*+m_1(t_0,t)+\frac{\bar{\omega}}{\delta_0},\end{aligned} \tag{31}$$

where $\bar{f}_1(x)=f_1(x)+\hat{\Psi}_{1,1}(x_1)+\hat{\Psi}_{1,2}(x_1,r)+(\sigma-\sigma_1+2)z_1^{\sigma-\sigma_1+1}\tanh^{\sigma-\sigma_1+2}\left(\frac{z_1}{\mu}\right)\frac{x_1^2\lambda(x_1^2)}{\delta_0}+\frac{3}{4}z_1^{\sigma-\sigma_1+1}$.

Based on Lemma 6, the unknown smooth nonlinear function $f_1(\cdot)$ is approximated using a fuzzy logic system (FLS) expressed in the form

$$\bar{f}_1(Z_1)=W_1^{*T}\Phi_1(Z_1)+\varepsilon_1(Z_1), \tag{32}$$

where $Z_1 = [x_1, x_2, \ldots, x_h]^T$ is the FLS input vector, W_1^* denotes the ideal weight vector, and $\varepsilon_1(Z_1)$ represents the fuzzy approximation error satisfying $\|\varepsilon_1(Z_1)\| \le \varepsilon_1^*$, with $\varepsilon_1^* > 0$ being a known constant.

By applying Young's inequality together with Lemma 7, the following bounds can be established:

$$\begin{aligned} z_1^{\sigma-\sigma_1+1} f_1 &\le |z_1|^{\sigma-\sigma_1+1}(\|W_1^*\|\,\|\Phi_1(Z_1)\| + \varepsilon_1^*) \\ &\le |z_1|^{\sigma-\sigma_1+1}(\|W_1^*\|\,\|\Phi_1(\chi_1)\| + \varepsilon_1^*) \\ &\le \frac{1}{2d_1^2} z_1^{2(\sigma-\sigma_1+1)} \Theta_1^* \Phi_1^T(\chi_1)\Phi_1(\chi_1) + \frac{d_1^2}{2} + \frac{1}{2} z_1^{2(\sigma-\sigma_1+1)} + \frac{\varepsilon_1^{*2}}{2} \end{aligned} \tag{33}$$

where $\Theta_1^* = \|W_1^*\|^2$, $d_1 > 0$ is a design constant and $\varepsilon_1^* > 0$ denotes an unknown bound satisfying $\|\varepsilon_1\| \le \varepsilon_1^*$.

Using (26) in (24), one has

$$\begin{aligned} \dot{V}_1 \le\ & z_1^{\sigma-\sigma_1+1}\left[\frac{1}{2d_1^2} z_1^{\sigma-\sigma_1+1}\hat{\Theta}_1\Phi_1^T(\chi_1)\Phi_1(\chi_1) + x_2^{\sigma_1} - \alpha_1^{\sigma_1} + \alpha_1^{\sigma_1} - \dot{y}_r\right] \\ & - \frac{g_0^-}{\delta_0} r^{1+\frac{\zeta}{2}} - \frac{g_0^+}{\delta_0} r^{1-\frac{\zeta}{2}} + \frac{\tilde{\Theta}_1}{\tau_1}\left[\frac{\tau_1}{2d_1^2} z_1^{2(\sigma-\sigma_1+1)}\Phi_1^T(\chi_1)\Phi_1(\chi_1) - \dot{\hat{\Theta}}_1\right] \\ & + \left(1 - (\sigma-\sigma_1+2)\tanh^{\sigma-\sigma_1+2}\left(\frac{z_1}{\mu}\right)\right)\frac{x_1^2\lambda(x_1^2)}{\delta_0} + l_{1,1}^* + l_{1,2}^* + m_1(t_0,t) \\ & + \frac{d_1^2}{2} + \frac{\varepsilon_1^{*2}}{2} + \frac{\bar{\omega}}{\delta_0}. \end{aligned} \tag{34}$$

Furthermore, applying Young's inequality, for any $\iota = 1, 2, \ldots, h$ one has

$$2(\mathfrak{e}+\tilde{\mathfrak{e}})\tilde{\Theta}_\iota\hat{\Theta}_\iota \le -(\mathfrak{e}+\tilde{\mathfrak{e}})\tilde{\Theta}_\iota^2 + (\mathfrak{e}+\tilde{\mathfrak{e}})\Theta_\iota^{*2}. \tag{35}$$

The virtual control law α_1 and the adaptive update law for the parameter estimate $\hat{\Theta}_1$ are designed as

$$\alpha_1 = -\left(\frac{1}{2d_1^2} z_1^{\sigma-\sigma_1+1}\hat{\Theta}_1\Phi_1^T(\chi_1)\Phi_1(\chi_1) + \Gamma_1 z_1^{\sigma_1} + \frac{\beta_1\pi}{\zeta T_d} z_1^{(1+\frac{\zeta}{2})((\sigma+1)-(\sigma-\sigma_1+1)} - \dot{y}_r\right)^{\frac{1}{\sigma_1}}, \tag{36}$$

$$\dot{\hat{\Theta}}_1 = \tau_1\frac{1}{2d_1^2} z_1^{2(\sigma-\sigma_1+1)}\Phi_1^T(\chi_1)\Phi_1(\chi_1) - 2(\mathfrak{e}+\tilde{\mathfrak{e}})\hat{\Theta}_1, \tag{37}$$

where $\beta_1 = \frac{(3n)^{\zeta/2}}{(\sigma-\sigma_1+2)(1+\zeta/2)}$, $\bar{\beta}_1 = \frac{1}{(\sigma-\sigma_1+2)^{(1-\zeta/2)}}$, $\Gamma_1 = \frac{\bar{\beta}_1\pi}{\zeta T_d} + 1$, $\mathfrak{e} = \frac{(2-\zeta)(3n)^{\zeta/2}\pi}{(2+\zeta/2)\tau^{\zeta/2}\kappa\zeta T_d}$, $\tilde{\mathfrak{e}} = \frac{(2-\zeta)\pi^2}{2^{(2-\zeta/2)}\tau_\kappa^{-\zeta/2}\zeta T_d}$, and the initial condition satisfies $\hat{\Theta}_1(0) \ge 0$.

Using (35)–(37) in (34), one has

$$\begin{aligned} \dot{V}_1 \le\ & z_1^{\sigma-\sigma_1+1}(x_2^{\sigma_1} - \alpha_1^{\sigma_1}) - \Gamma_1 z_1^{\sigma+1} - \beta_1\frac{\pi}{\zeta T_d} z_1^{(\sigma+1)(1+\zeta/2)} - (\mathfrak{e}+\tilde{\mathfrak{e}})\frac{1}{\tau_1}\tilde{\Theta}_1^2 \\ & - \frac{g_0^-}{\delta_0} r^{1+\frac{\zeta}{2}} - \frac{g_0^+}{\delta_0} r^{1-\frac{\zeta}{2}} + (\mathfrak{e}+\tilde{\mathfrak{e}})\frac{1}{\tau_1}\Theta_1^{*2} \\ & + \left(1 - (\sigma-\sigma_1+2)\tanh^{\sigma-\sigma_1+2}\frac{z_1}{\mu}\right)\frac{x_1^2\lambda(x_1^2)}{\delta_0} + l_{1,1}^* + l_{1,2}^* + m_1(t_0,t) \\ & + \frac{d_1^2}{2} + \frac{\varepsilon_1^{*2}}{2} + \frac{\bar{\omega}}{\delta_0}. \end{aligned} \tag{38}$$

Using Lemmas 1 and 3, one has

$$\begin{aligned} z_1^{\sigma-\sigma_1+1}\left(x_2^{\sigma_1}-\alpha_1^{\sigma_1}\right) &\leq \sigma_1|z_1|^{\sigma-\sigma_1+1}|x_2-\alpha_1|\left(|x_2|^{\sigma_1-1}+|\alpha_1|^{\sigma_1-1}\right) \\ &\leq |z_1|^{\sigma+1}+\Delta_{11}|z_2|^{\sigma+1}+\Delta_{12}|z_2|^{(\sigma+1)/\sigma_1}, \end{aligned} \tag{39}$$

where $\Delta_{11} = \frac{2^{\sigma_1-1}\sigma_1^2}{\sigma+1}\left(\frac{\sigma+1}{\sigma-\sigma_1+1}\frac{1}{\sigma_1 2^{\sigma_1}}\right)^{-\frac{\sigma-\sigma_1+1}{\sigma_1}}$ is a positive constant related to the given constants σ and σ_1 and $\Delta_{12} = \frac{\sigma_1^2(2^{\sigma_1-1}+1)}{\sigma+1}\left(\frac{\sigma+1}{\sigma-\sigma_1+1}\frac{1}{\sigma_1(2^{\sigma_1}+2)}\right)^{-\frac{\sigma-\sigma_1+1}{\sigma_1}}\alpha^{\frac{(\sigma_1-1)(\sigma+1)}{\sigma_1}}$ is a non-negative function.

Using (39) in (38), one has

$$\begin{aligned} \dot{V}_1 \leq & -\beta_1\frac{\pi}{\zeta T_d}z_1^{(\sigma+1)(1+\zeta/2)}-\bar{\beta}_1\frac{\pi}{\zeta T_d}z_1^{(\sigma+1)(1-\zeta/2)}-\Gamma_1 z_1^{\sigma+1} \\ & -(\mathfrak{e}+\tilde{\mathfrak{e}})\frac{1}{\tau_1}\tilde{\Theta}_1^2-\frac{g_0^-}{\delta_0}r_1^{1+\zeta/2}-\frac{g_0^+}{\delta_0}r_1^{1-\zeta/2}+\Delta_{11}z_2^{\sigma+1}+\Delta_{12}z_2^{(\sigma+1)/\sigma_1} \\ & +\frac{\bar{\omega}}{\delta_0}+\left(1-(\sigma-\sigma_1+2)\tanh^{\sigma-\sigma_1+2}\frac{z_1}{\mu}\right)\frac{x_1^2\lambda(x_1^2)}{\delta_0}+l_{1,1}^*+l_{1,2}^*+m_1(t_0,t) \\ & +(\mathfrak{e}+\tilde{\mathfrak{e}})\frac{1}{\tau_1}\Theta_1^{*2}+\frac{d_1^2}{2}+\frac{\varepsilon_1^{*2}}{2}+\frac{\bar{\beta}_1\pi}{\zeta T_d}z_1^{\left(1-\frac{\zeta}{2}\right)(\sigma+1)}. \end{aligned} \tag{40}$$

Applying Lemma 1, one has

$$z_1^{(\sigma+1)(1-\zeta/2)} \leq \frac{\zeta T_d\bar{\Gamma}_1}{\bar{\beta}_1\pi}z_1^{(\sigma+1)}+\frac{\zeta}{2}\left(\frac{\zeta T_d\bar{\Gamma}_1}{(1-\zeta/2)\bar{\beta}_1\pi}\right)^{1-2/\zeta}. \tag{41}$$

Next, the time derivative of V_1 can be calculated as

$$\begin{aligned} \dot{V}_1 \leq & -\beta_1\frac{\pi}{\zeta T_d}z_1^{(\sigma+1)(1+\zeta/2)}-\bar{\beta}_1\frac{\pi}{\zeta T_d}z_1^{(\sigma+1)(1-\zeta/2)} \\ & -(\mathfrak{e}+\tilde{\mathfrak{e}})\frac{1}{\tau_1}\tilde{\Theta}_1^2-\frac{g_0^-}{\delta_0}r_1^{1+\zeta/2}-\frac{g_0^+}{\delta_0}r_1^{1-\zeta/2}+\Delta_{11}z_2^{\sigma+1}+\Delta_{12}z_2^{(\sigma+1)/\sigma_1} \\ & +\frac{\bar{\omega}}{\delta_0}+\left(1-(\sigma-\sigma_1+2)\tanh^{\sigma-\sigma_1+2}\frac{z_1}{\mu}\right)\frac{x_1^2\lambda(x_1^2)}{\delta_0}+l_{1,1}^*+l_{1,2}^*+m_1(t_0,t) \\ & +(\mathfrak{e}+\tilde{\mathfrak{e}})\frac{1}{\tau_1}\Theta_1^{*2}+\frac{d_1^2}{2}+\frac{\varepsilon_1^{*2}}{2}+\frac{\bar{\beta}_1\pi}{\zeta T_d}\left(\frac{\zeta T_d\bar{\Gamma}_1}{(1-\zeta/2)\bar{\beta}_1\pi}\right)^{1-2/\zeta}. \end{aligned} \tag{42}$$

Setting $\mathcal{P} = z_\iota$, $\mathcal{N} = j$, $\tilde{c} = \mathcal{D}(\sigma-\sigma_\iota+2)$, $\tilde{d} = \mathcal{D}(\sigma+1)-\mathcal{D}(\sigma-\sigma_\iota+2)$, $\epsilon = \frac{\sigma+1}{\sigma-\sigma_\iota+2}$, one obtains

$$-z_\iota^{\mathcal{D}(\sigma+1)} \leq -z_\iota^{\mathcal{D}(\sigma-\sigma_\iota+2)}j^{\mathcal{D}(\sigma_\iota-1)}+\frac{\sigma_\iota-1}{\sigma+1}\left[\frac{\sigma+1}{\sigma-\sigma_\iota+2}\right]^{-(\sigma-\sigma_\iota+2)/(\sigma_\iota-1)}j^{\mathcal{D}(\sigma+1)}, \tag{43}$$

where $\mathcal{D} > 0$ and $j > 0$ are positive constants.

For (43), let us set $\iota = 1, 2, \ldots, \hbar$. Defining $\mathcal{D} = 1+\zeta/2$ and $j = 1$, we obtain

$$-z_\iota^{(\sigma+1)(1+\zeta/2)} \leq -z_\iota^{(\sigma-\sigma_\iota+2)(1+\zeta/2)}+\frac{\sigma_\iota-1}{\sigma+1}\left[\frac{\sigma+1}{\sigma-\sigma_\iota+2}\right]^{-(\sigma-\sigma_\iota+2)/(\sigma_\iota-1)}. \tag{44}$$

Similarly, for $\iota = 1, 2, \ldots, \hbar$, if we choose $\mathcal{D} = 1-\zeta/2$ and $j = 1$, we have

$$-z_\iota^{(\sigma+1)(1-\zeta/2)} \leq -z_\iota^{(\sigma-\sigma_\iota+2)(1-\zeta/2)}+\frac{\sigma_\iota-1}{\sigma+1}\left[\frac{\sigma+1}{\sigma-\sigma_\iota+2}\right]^{-(\sigma-\sigma_\iota+2)/(\sigma_\iota-1)}. \tag{45}$$

Using (43)–(45) in (42), one has

$$\dot{V}_1 \leq -\beta_1\frac{\pi}{\zeta T_d}z_1^{(\sigma-\sigma_1+2)(1+\zeta/2)} - \bar{\beta}_1\frac{\pi}{\zeta T_d}z_1^{(\sigma-\sigma_1+2)(1-\zeta/2)} - (\mathfrak{e}+\tilde{\mathfrak{e}})\frac{1}{\tau_1}\tilde{\Theta}_1^2 - \frac{g_0^-}{\delta_0}r_1^{1+\zeta/2} - \frac{g_0^+}{\delta_0}r_1^{1-\zeta/2} + \Delta_{11}z_2^{\sigma+1} + \Delta_{12}z_2^{(\sigma+1)/\sigma_1} + M_1 + \left(1-(\sigma-\sigma_1+2)\tanh^{\sigma-\sigma_1+2}\frac{z_1}{\mu}\right)\frac{x_1^2\lambda(x_1^2)}{\delta_0}, \tag{46}$$

where $M_1 = (\beta_1+\bar{\beta}_1)\frac{\pi}{\zeta T_d}\frac{\sigma_1-1}{\sigma+1}\left[\frac{\sigma+1}{\sigma-\sigma_1+2}\right]^{-(\sigma-\sigma_1+2)/(\sigma_1-1)} + l_{1,1}^* + l_{1,2}^* + m_1(t_0,t) + (\mathfrak{e}+\tilde{\mathfrak{e}})\frac{1}{\tau_1}\Theta_1^{*2} + \frac{d_1^2}{2} + \frac{\varepsilon_1^{*2}}{2} + \frac{\omega}{\delta_0} + \beta_1\frac{\pi}{2T_d}\left(\frac{\zeta T_d\Gamma_1}{(1-\zeta/2)\beta_1\pi}\right)^{1-2/\zeta}$.

Step ι ($\iota = 2,3,\ldots,\hbar-1$): Using (1) and (18), the derivative of z_ι is

$$\dot{z}_\iota = x_{\iota+1}^{\sigma_\iota} + f_\iota(x) + \Delta_\iota - \dot{\alpha}_{\iota-1}, \tag{47}$$

where

$$\dot{\alpha}_{\iota-1} = \sum_{\kappa=1}^{\iota-1}\frac{\partial\alpha_{\iota-1}}{\partial x_\kappa}x_{\kappa+1} + \sum_{\kappa=1}^{\iota-1}\frac{\partial\alpha_{\iota-1}}{\partial x_\kappa}f_\kappa + \sum_{\kappa=1}^{\iota-1}\frac{\partial\alpha_{\iota-1}}{\partial x_\kappa}\Delta_\kappa + \sum_{\kappa=1}^{\iota-1}\frac{\partial\alpha_{\iota-1}}{\partial\hat{\Theta}_\kappa}\dot{\hat{\Theta}}_\kappa + \sum_{\kappa=0}^{\iota-1}\frac{\partial\alpha_{\iota-1}}{\partial y^{(\kappa)}}r^{(\kappa+1)} + \frac{\partial\alpha_{\iota-1}}{\partial r}\dot{r}. \tag{48}$$

Consider the following Lyapunov function as

$$V_\iota = V_{\iota-1} + \frac{z_\iota^{\sigma-\sigma_\iota+2}}{\sigma-\sigma_\iota+2} + \frac{\tilde{\Theta}_\iota^2}{2\tau_\iota}, \tag{49}$$

where $\hat{\Theta}_\iota$ is the estimate of Θ_ι^*, $\tilde{\Theta}_\iota = \Theta_\iota^* - \hat{\Theta}_\iota$, and $\tau_\iota > 0$ is a designed parameter.

Let $\bar{\Delta}_\iota$ be defined as $\bar{\Delta}_\iota = \Delta_\iota - \sum_{\kappa=1}^{\iota-1}\frac{\partial\alpha_{\iota-1}}{\partial x_\kappa}\Delta_\kappa$. By invoking Assumption 2 together with Lemmas 2 and 5 and applying arguments similar to those presented in Step 1, we have

$$z_\iota^{\sigma-\sigma_\iota+1}\bar{\Delta}_\iota \leq z_\iota^{\sigma-\sigma_\iota+1}\hat{\Psi}_{\iota,1}(x_1,\ldots,x_\iota) + z_\iota^{\sigma-\sigma_\iota+1}\hat{\Psi}_{\iota,2}(x_1,\ldots,x_\iota,r) + l_{\iota,1}^* + l_{\iota,2}^* + \frac{1}{4}z_\iota^{2(\sigma-\sigma_\iota+1)} + m_\iota(t_0,t), \tag{50}$$

where $l_{\iota,1} > 0$, $l_{\iota,2} > 0$, $\hat{\Psi}_{\iota,1} = \left(\Psi_{\iota,1} + \sum_{\kappa=1}^{\iota-1}\left|\frac{\partial\alpha_{\iota-1}}{\partial x_\kappa}\right|\Psi_{\iota,1}\right)\tanh\left(\frac{z_\iota^{\sigma-\sigma_{\iota+1}}}{l_{\iota,1}}\left(\Psi_{\iota,1} + \sum_{\kappa=1}^{\iota-1}\left|\frac{\partial\alpha_{\iota-1}}{\partial x_\kappa}\right|\Psi_{\iota,1}\right)\right)$, $l_{\iota,1}^* = 0.2785\,l_{\iota,1}$, $\Psi_{\iota,2}(x_1,x_2,\ldots,x_\iota,r) = \Psi_{\iota,2}\circ\mathcal{L}^{-1}(2r) + \sum_{\kappa=1}^{\iota-1}\left|\frac{\partial\alpha_{\iota-1}}{\partial x_\kappa}\right|\Psi_{\iota,1}\,\Psi_{\iota,2}\circ\mathcal{L}^{-1}(2r)$, $\hat{\Psi}_{\iota,2}(x_1,x_2,\ldots,x_\iota,r) = \Psi_{\iota,2}(x_1,x_2,\ldots,x_\iota,r)\tanh\left(\frac{z_\iota^{\sigma-\sigma_{\iota+1}}}{l_{\iota,2}}\Psi_{\iota,2}(x_1,x_2,\ldots,x_\iota,r)\right)$, $m_\iota(t_0,t) = \sum_{\kappa=1}^{\iota}\left(\Psi_{\kappa,2}\circ\mathcal{L}^{-1}(2M(t_0,t))\right)^2$, and $m_\iota(t_0,t) \geq 0$ for all $t \geq t_0+T_0$, $l_{\iota,2}^* = 0.2785\,l_{\iota,2}$.

Using the results given in (47)–(50), the time derivative of V_ι can be expressed as

$$\begin{aligned}\dot{V}_\iota \leq & -\sum_{\kappa=1}^{\iota-1}\frac{\beta_\kappa\pi}{\varsigma T_d}z_\kappa^{(1+\varsigma/2)(\sigma-\sigma_\kappa+2)} - \sum_{\kappa=1}^{\iota-1}\beta_\kappa\frac{\bar{\beta}_\kappa\pi}{\varsigma T_d}z_\kappa^{(1-\varsigma/2)(\sigma-\sigma_\kappa+2)} - \sum_{\kappa=1}^{\iota-1}\frac{\mathfrak{e}+\tilde{\mathfrak{e}}}{\tau_\kappa}\tilde{\Theta}_\kappa^2 \\ & + \Delta_{(\iota-1)1}z_\iota^{\sigma+1} + \Delta_{(\iota-1)2}z_\iota^{(\sigma+1)/\sigma_\iota} - \frac{1}{\tau_\iota}\tilde{\Theta}_\iota\dot{\hat{\Theta}}_\iota - \frac{1}{2}z_\iota^{2(\sigma-\sigma_\iota+1)} \\ & - g_0\delta_0 r_1^{+(1+\varsigma)/2} - g_0\delta_0 r_1^{-(1-\varsigma)/2} + \left(1-(\sigma-\sigma_1+2)\tanh^{\sigma-\sigma_1+2}\frac{z_1}{\mu}\right)x_1^2\lambda(x_1)\delta_0 \\ & + l_{\iota,1}^* + l_{\iota,2}^* + m_\iota(t_0,t) + M_{\iota-1} \\ & + z_\iota^{\sigma-\sigma_\iota+1}\left(x_{\iota+1}^{\sigma_\iota} + \bar{f}_\iota(x) - \sum_{\kappa=1}^{\iota-1}\frac{\partial\alpha_{\iota-1}}{\partial x_\kappa}x_{\kappa+1} - \sum_{\kappa=1}^{\iota-1}\frac{\partial\alpha_{\iota-1}}{\partial x_\kappa}f_\kappa\right. \\ & \left. - \sum_{\kappa=1}^{\iota-1}\frac{\partial\alpha_{\iota-1}}{\partial\hat{\Theta}_\kappa}\dot{\hat{\Theta}}_\kappa - \sum_{\kappa=0}^{\iota-1}\frac{\partial\alpha_{\iota-1}}{\partial y^{(\kappa)}}r^{(\kappa+1)} - \frac{\partial\alpha_{\iota-1}}{\partial r}\dot{r}\right),\end{aligned} \tag{51}$$

where $\bar{f}_\iota(x) = f_\iota(x) + \frac{3}{4}z_\iota^{\sigma-\sigma_\iota+1} + \hat{\Psi}_{\iota,1}(x_1,\ldots,x_\iota) + \hat{\Psi}_{\iota,2}(x_1,\ldots,x_\iota,r)$.

Now, $\bar{f}_\iota$ can be estimated through a fuzzy logic system (FLS) approximation of the form

$$\bar{f}_\iota(Z_\iota) = W_\iota^{*T}\Phi_\iota(Z_\iota) + \varepsilon_\iota(Z_\iota), \quad \|\varepsilon_\iota(Z_\iota)\| \le \varepsilon_\iota^*, \tag{52}$$

where $Z_\iota = [x_1,\ldots,x_h,\hat{\Theta}_1,\ldots,\hat{\Theta}_{\iota-1}]^T$ and $\varepsilon_\iota^* > 0$ is a constant.

With the help of Young's inequality and Lemma 7, we have

$$\begin{aligned} z_\iota^{\sigma-\sigma_\iota+1}f_\iota &\le |z_\iota|^{\sigma-\sigma_\iota+1}\left(\|W_\iota^*\|\,\|\Phi_\iota(Z_\iota)\| + \varepsilon_\iota^*\right) \\ &\le \frac{1}{2d_\iota^2}z_\iota^{2(\sigma-\sigma_\iota+1)}\Theta_\iota^*\Phi_\iota^T(\chi_\iota)\Phi_\iota(\chi_\iota) + \frac{d_\iota^2}{2} + \frac{1}{2}z_\iota^{2(\sigma-\sigma_\iota+1)} + \frac{(\varepsilon_\iota^*)^2}{2}, \end{aligned} \tag{53}$$

where $\Theta_\iota^* = \|W_\iota^*\|^2$, $\chi_\iota = [x_1,\ldots,x_\iota]^T$, $d_\iota > 0$ is a design parameter and $\varepsilon_\iota^* > 0$ satisfies $\|\varepsilon_\iota\| \le \varepsilon_\iota^*$.

The virtual controller α_ι and the adaptive law for $\hat{\Theta}_\iota$ are designed as

$$\begin{aligned} \alpha_\iota = -\frac{1}{\sigma_\iota}\Bigg(&\frac{1}{2d_\iota^2}z_\iota^{\sigma-\sigma_\iota+1}\Theta_\iota\Phi_\iota^T(\chi_\iota)\Phi_\iota(\chi_\iota) + \Delta_{(\iota-1)1}z_\iota^{\sigma_\iota} + \Delta_{(\iota-1)2}z_\iota^{\sigma_\iota} \\ &- \sum_{\kappa=1}^{\iota-1}\frac{\partial\alpha_{\iota-1}}{\partial x_\kappa}x_{\kappa+1} - \sum_{\kappa=1}^{\iota-1}\frac{\partial\alpha_{\iota-1}}{\partial x_\kappa}f_\kappa - \sum_{\kappa=1}^{\iota-1}\frac{\partial\alpha_{\iota-1}}{\partial\hat{\Theta}_\kappa}\dot{\hat{\Theta}}_\kappa \\ &- \sum_{\kappa=0}^{\iota-1}\frac{\partial\alpha_{\iota-1}}{\partial y^{(\kappa)}}r^{(\kappa+1)} - \frac{\partial\alpha_{\iota-1}}{\partial r}\dot{r} + \Gamma_\iota z_\iota^{\sigma_\iota} + \frac{\beta_\iota\pi}{\varsigma T_d}z_\iota^{(1+\varsigma/2)(\sigma+1)-(\sigma-\sigma_\iota+1)}\Bigg)^{\frac{1}{\sigma_\iota}}, \end{aligned} \tag{54}$$

$$\dot{\hat{\Theta}}_\iota = \tau_\iota\frac{1}{2d_\iota^2}z_\iota^{2(\sigma-\sigma_\iota+1)}\Phi_\iota^T(\chi_\iota)\Phi_\iota(\chi_\iota) - 2(\mathfrak{e}+\tilde{\mathfrak{e}})\hat{\Theta}_\iota, \tag{55}$$

where $\beta_\iota = \frac{(3n)^{\frac{\varsigma}{2}}}{(\sigma-\sigma_\iota+2)(1+\varsigma/2)}$, $\bar{\beta}_\iota = \frac{1}{(\sigma-\sigma_\iota+2)^{(1-\varsigma/2)}}$, and $\Gamma_\iota = \frac{\bar{\beta}_\iota\pi}{\varsigma T_d} + 1$. Moreover, $\bar{\sigma}_\iota = \frac{\sigma+1}{\sigma_{\iota-1}} - (\sigma-\sigma_\iota+1)$, $\hat{\Theta}_\iota(0) \ge 0$, and σ_ι is a non-negative constant under Assumption 3.

In addition, $\Delta_{(\iota-1)1} = \frac{\sigma_{\iota-1}^{2\sigma_{\iota-1}-1}}{\sigma+1}\left[\frac{\sigma+1}{\sigma_{\iota-1}2^{\sigma_{\iota-1}}(\sigma-\sigma_{\iota-1}+1)}\right]^{-\frac{\sigma-\sigma_{\iota-1}+1}{\sigma_{\iota-1}}}$

and $\Delta_{(\iota-1)2} = \frac{\sigma_{\iota-1}^2(2^{\sigma_{\iota-1}-1}+1)}{\sigma+1}\alpha^{(\sigma_{\iota-1}-1)(\sigma+1)/\sigma_{\iota-1}}\left[\frac{\sigma+1}{\sigma_{\iota-1}(\sigma-\sigma_{\iota-1}+1)(2\sigma_{\iota-1}+2)}\right]^{-\frac{\sigma-\sigma_{\iota-1}+1}{\sigma_{\iota-1}}}$.

Using (53)–(55) in (51), one has

$$\begin{aligned} \dot{V}_\iota \le &-\sum_{\kappa=1}^{\iota-1}\frac{\beta_\kappa\pi}{\varsigma T_d}z_\kappa^{(1+\varsigma/2)(\sigma-\sigma_\kappa+2)} - \sum_{\kappa=1}^{\iota-1}\beta_\kappa\frac{\pi\varsigma}{T_d}z_\kappa^{(1-\varsigma/2)(\sigma-\sigma_\kappa+2)} - \sum_{\kappa=1}^{\iota}\frac{\mathfrak{e}+\tilde{\mathfrak{e}}}{\tau_\kappa}\tilde{\Theta}_\kappa^2 \\ &+ z_\iota^{\sigma-\sigma_\iota+1}(x_{\iota+1}^{\sigma_\iota} - \alpha_\iota^{\sigma_\iota}) - \Gamma_\iota z_\iota^{\sigma+1} - \frac{\beta_\iota\pi}{\varsigma T_d}z_\iota^{(1+\varsigma/2)(\sigma+1)} - \frac{\beta_\iota\,\pi}{\varsigma T_d}z_\iota^{(1-\varsigma/2)(\sigma+1)} \\ &+ \frac{(\mathfrak{e}+\tilde{\mathfrak{e}})}{2\tau_\iota}\Theta_\iota^{*2} - \frac{g_0}{\delta_0}r_1^{(1+\varsigma/2)} - \frac{\bar{g}_0}{\delta_0}r_1^{(1-\varsigma/2)} + \frac{\beta_\iota\pi}{\varsigma T_d}z_\iota^{(1-\varsigma/2)(\sigma+1)} + m_\iota(t_0,t) \\ &+ \left(1-(\sigma-\sigma_1+2)\tanh^{\sigma-\sigma_1+2}(z_1/\mu)\right)x_1^2\lambda(x_1^2) + M_{\iota-1} + l_{\iota,1}^* + l_{\iota,2}^* + \frac{d_\iota^2}{2} + \frac{(\varepsilon_\iota^*)^2}{2}. \end{aligned} \tag{56}$$

Per Lemmas 1 and 3, one has

$$z_\iota^{\sigma-\sigma_\iota+1}\left(x_{\iota+1}^{\sigma_\iota} - \alpha_\iota^{\sigma_\iota}\right) \le z_\iota^{\sigma+1} + \Delta_{\iota1}z_{\iota+1}^{\sigma+1} + \Delta_{\iota2}z_{\iota+1}^{\frac{\sigma_\iota+1}{\sigma_\iota}}. \tag{57}$$

where $\Delta_{\iota1} = \frac{2^{\sigma_\iota-1}\sigma_\iota^2}{\sigma+1}\left(\frac{\sigma+1}{(\sigma-\sigma_\iota+1)\sigma_\iota 2^{\sigma_\iota}}\right)^{-\frac{\sigma-\sigma_\iota+1}{\sigma_\iota}}$, which is a positive constant related to the given constants σ and σ_ι, and $\Delta_{\iota2} = \frac{\sigma_\iota^2(2^{\sigma_\iota-1}+1)}{\sigma+1}\left(\frac{\sigma+1}{(\sigma-\sigma_\iota+1)\sigma_\iota(2^{\sigma_\iota+1}+2)}\right)^{-\frac{\sigma-\sigma_\iota+1}{\sigma_\iota}}\alpha^{\frac{(\sigma_\iota-1)(\sigma+1)}{\sigma_\iota}}$, where α is a nonnegative function.

Furthermore, by Lemma 1, we have

$$z_\iota^{(1-\varsigma/2)(\sigma+1)} \leq \frac{\varsigma T_d \bar{\Gamma}_\iota}{\bar{\beta}_\iota \pi} z_\iota^{\sigma+1} + \frac{\varsigma}{2}\left(\frac{\varsigma T_d \bar{\Gamma}_\iota}{(1-\varsigma/2)\bar{\beta}_\iota \pi}\right)^{1-2/\varsigma}, \tag{58}$$

where $\Gamma_\iota = \Gamma_\iota - 1$.

Using (57) and (58) in (56), one has

$$\begin{aligned}\dot{V}_\iota \leq & -\sum_{\kappa=1}^{\iota-1} \frac{\beta_\kappa \pi}{\varsigma T_d} z_\kappa^{(1+\varsigma/2)(\sigma-\sigma_\kappa+2)} - \sum_{\kappa=1}^{\iota-1} \frac{\bar{\beta}_\kappa \pi}{\varsigma T_d} z_\kappa^{(1-\varsigma/2)(\sigma-\sigma_\kappa+2)} - \sum_{\kappa=1}^{\iota} \frac{\mathfrak{e}+\tilde{\mathfrak{e}}}{\tau_\kappa}\tilde{\Theta}_\kappa^2 \\ & - \frac{g_0}{\delta_0} r_1^{1+\varsigma/2} - \frac{g_0}{\delta_0} r_1^{1-\varsigma/2} + \Delta_{\iota 1} z_{\iota+1}^{\sigma+1} + \Delta_{\iota 2} z_{\iota+1}^{\frac{\sigma+1}{\sigma_\iota}} + M_{\iota-1} + l_{\iota,1}^* + l_{\iota,2}^* \\ & + \left(1 - (\sigma - \sigma_1 + 2)\tanh^{\sigma-\sigma_1+2}\frac{z_1}{\mu}\right)\frac{x_1^2 \lambda(x_1^2)}{\delta_0} + \frac{\bar{\beta}_\iota \pi}{2T_d}\left(\frac{\varsigma T_d \bar{\Gamma}_\iota}{(1-\varsigma/2)\bar{\beta}_\iota \pi}\right)^{1-2/\varsigma} \\ & + m_\iota(t_0, t) + \frac{(\mathfrak{e}+\tilde{\mathfrak{e}})\Theta_\iota^{*2}}{2\tau_\iota} + \frac{d_\iota^2}{2} + \frac{(\varepsilon_\iota^*)^2}{2}.\end{aligned} \tag{59}$$

Using (44) and (45) into (59), one has

$$\begin{aligned}\dot{V}_\iota \leq & \sum_{\kappa=1}^{\iota-1} \frac{\beta_\kappa \pi}{\varsigma T_d} z_\kappa^{(1+\varsigma/2)(\sigma-\sigma_\kappa+2)} - \sum_{\kappa=1}^{\iota-1} \frac{\bar{\beta}_\kappa \pi}{\varsigma T_d} z_\kappa^{(1-\varsigma/2)(\sigma-\sigma_\kappa+2)} - \sum_{\kappa=1}^{\iota} \frac{\mathfrak{e}+\tilde{\mathfrak{e}}}{\tau_\kappa}\tilde{\Theta}_\kappa^2 \\ & - \frac{g_0}{\delta_0} r_1^{1+\varsigma/2} - \frac{g_0}{\delta_0} r_1^{1-\varsigma/2} + \Delta_{\iota 1} z_{\iota+1}^{\sigma+1} + \Delta_{\iota 2} z_{\iota+1}^{\frac{\sigma+1}{\sigma_\iota}} + M_\iota \\ & + \left(1 - (\sigma - \sigma_1 + 2)\tanh^{\sigma-\sigma_1+2}\frac{z_1}{\mu}\right)\frac{x_1^2 \lambda(x_1^2)}{\delta_0},\end{aligned} \tag{60}$$

where $M_\iota = m_\iota(t_0, t) + \frac{(\mathfrak{e}+\tilde{\mathfrak{e}})\Theta_\iota^{*2}}{2\tau_\iota} + \frac{\bar{\beta}_\iota \pi}{2T_d}\left(\frac{\varsigma T_d \bar{\Gamma}_\iota}{(1-\varsigma/2)\bar{\beta}_\iota \pi}\right)^{1-2/\varsigma} + \frac{(\beta_\iota + \bar{\beta}_\iota)\pi}{\varsigma T_d}\frac{\sigma_\iota - 1}{\sigma+1}\left[\frac{\sigma+1}{\sigma-\sigma_\iota+2}\right]^{-\frac{\sigma-\sigma_\iota+2}{\sigma_\iota-1}} + l_{\iota,1}^* + l_{\iota,2}^* + \frac{d_\iota^2}{2} + \frac{(\varepsilon_\iota^*)^2}{2} + M_{\iota-1}$.

Step h**:** Using (8) and (25), one has

$$\begin{aligned}\dot{z}_h &= \dot{x}_h - \dot{\alpha}_{h-1} + \frac{\dot{x}_{h+1}}{\lambda} \\ &= x_{h+1} - u^{\sigma_h} - \dot{\alpha}_{h-1} + f_h(x) + \Delta_h + \frac{1}{\lambda}(-\lambda x_{h+1} + 2\lambda u^{\sigma_h}), \\ &= u^{\sigma_h} + f_h(x) + \Delta_h - \dot{\alpha}_{h-1},\end{aligned} \tag{61}$$

where $\dot{\alpha}_{h-1}$ is defined analogously to $\dot{\alpha}_{\iota-1}$ in Step ι.

Consider the following Lyapunov function as

$$V_h = V_{h-1} + \frac{z_h^{\sigma-\sigma_h+2}}{\sigma-\sigma_h+2} + \frac{\tilde{\Theta}_h^2}{2\tau_h}, \tag{62}$$

where $\hat{\Theta}_h$ is the estimation of Θ_h^*, $\tilde{\Theta}_h = \Theta_h^* - \hat{\Theta}_h$, and $\tau_h > 0$ is a designed positive parameter.

Define $\Delta_h = \bar{\Delta}_h - \sum_{\kappa=1}^{h-1} \frac{\partial \alpha_{h-1}}{\partial x_\kappa}\Delta_\kappa$. Similar to Step 1, one has

$$\begin{aligned}z_h^{\sigma-\sigma_h+1}\bar{\Delta}_h \leq & z_h^{\sigma-\sigma_h+1}\hat{\Psi}_{h,1}(x_1, \ldots, x_h) + z_h^{\sigma-\sigma_h+1}\hat{\Psi}_{h,2}(x_1, \ldots, x_h, r) \\ & + l_{h,1}^* + l_{h,2}^* + \frac{1}{4} z_h^{2(\sigma-\sigma_h+1)} + m_h(t_0, t),\end{aligned} \tag{63}$$

where $l_{h,1} > 0, \quad l_{h,2} > 0, \hat{\Psi}_{h,1} = \left(\Psi_{h,1} + \sum_{\kappa=1}^{h-1}\left|\frac{\partial \alpha_{h-1}}{\partial x_\kappa}\right|\Psi_{h,1}\right)\tanh\left(\frac{z_h^{\sigma-\sigma_{h+1}}}{l_{h,1}}\left(\Psi_{h,1} + \sum_{\kappa=1}^{h-1}\left|\frac{\partial \alpha_{h-1}}{\partial x_\kappa}\right|\Psi_{h,1}\right)\right)$, $l_{h,1}^* = 0.2785\, l_{h,1}$, $\Psi_{h,2}(x_1, x_2, \ldots, x_h, r) = \Psi_{h,2} \circ \mathcal{L}^{-1}(2r) + \sum_{\kappa=1}^{h-1}\left|\frac{\partial \alpha_{h-1}}{\partial x_\kappa}\right|\Psi_{h,1}\, \Psi_{h,2} \circ \mathcal{L}^{-1}(2r)$,

$$\hat{\Psi}_{h,2}(x_1, x_2, \ldots, x_h, r) = \Psi_{h,2}(x_1, x_2, \ldots, x_h, r) \tanh\left(\frac{z_h^{\sigma-\sigma_{h+1}}}{l_{h,2}} \Psi_{h,2}(x_1, x_2, \ldots, x_h, r)\right),$$

$m_h(t_0, t) = \sum_{\kappa=1}^{h} \left(\Psi_{\kappa,2} \circ \mathcal{L}^{-1}(2M(t_0, t))\right)^2$, $m_h(t_0, t) \geq 0$ for all $t \geq t_0 + T_0$.

Using (63) and differentiating V_h, one has

$$\begin{aligned}
\dot{V}_h \leq & -\sum_{\kappa=1}^{h-1} \frac{\beta_\kappa \pi}{\varsigma T_d} z_\kappa^{(1+\varsigma/2)(\sigma-\sigma_\kappa+2)} - \sum_{\kappa=1}^{h-1} \frac{\bar{\beta}_\kappa \pi}{\varsigma T_d} z_\kappa^{(1-\varsigma/2)(\sigma-\sigma_\kappa+2)} - \sum_{\kappa=1}^{h-1} \frac{\mathfrak{e}+\tilde{\mathfrak{e}}}{\tau_\kappa} \tilde{\Theta}_\kappa^2 \\
& - \frac{1}{\tau_h} \tilde{\Theta}_h \dot{\hat{\Theta}}_h - \frac{g_0}{\delta_0} r_1^{+(1+\varsigma)/2} - \frac{\bar{g}_0}{\delta_0} r_1^{-(1-\varsigma)/2} \\
& + \left(1 - (\sigma - \sigma_1 + 2) \tanh^{\sigma-\sigma_1+2} \frac{z_1}{\mu}\right) x_1^2 \lambda(x_1) \delta_0 \\
& + l_{h,1}^* + l_{h,2}^* + m_h(t_0, t) + M_{h-1} + z_h^{\sigma-\sigma_h+1} \left(u^{\sigma_h} + \bar{f}_h(x)\right),
\end{aligned} \tag{64}$$

where $\bar{\sigma}_h = \dfrac{\sigma+1}{\sigma_{h-1}} - (\sigma - \sigma_h + 1)$ denotes a non-negative constant and

$$\begin{aligned}
\bar{f}_h(x) = & f_h(x) + \Delta_{(h-1)1} z_h^{\sigma_h} + \Delta_{(h-1)2} z_h^{\bar{\sigma}_h} + \hat{\Psi}_{h,1}(x) + \hat{\Psi}_{h,2}(x, r) + \frac{3}{4} z_h^{\sigma-\sigma_h+1} \\
& - \sum_{\kappa=1}^{h-1} \frac{\partial \alpha_{h-1}}{\partial x_\kappa} x_{\kappa+1} - \sum_{\kappa=1}^{h-1} \frac{\partial \alpha_{h-1}}{\partial x_\kappa} f_\kappa - \sum_{\kappa=1}^{h-1} \frac{\partial \alpha_{h-1}}{\partial \hat{\Theta}_\kappa} \dot{\hat{\Theta}}_\kappa \\
& - \sum_{\kappa=0}^{h-1} \frac{\partial \alpha_{h-1}}{\partial y^{(\kappa)}} r^{(\kappa+1)} - \frac{\partial \alpha_{h-1}}{\partial r} \dot{r}.
\end{aligned} \tag{65}$$

Now, $\bar{f}_h$ can be approximated by the FLS as

$$\bar{f}_h(Z_h) = W_h^{*T} \Phi_h(Z_h) + \varepsilon_h(Z_h), \quad \|\varepsilon_h(Z_h)\| \leq \varepsilon_h^*, \tag{66}$$

where $Z_h = [x_1, \ldots, x_h, \hat{\Theta}_1, \ldots, \hat{\Theta}_{h-1}]^T$, and $\varepsilon_h^* > 0$ is a constant.

With the help of Young's inequality and Lemma 7, one has

$$\begin{aligned}
z_h^{\sigma-\sigma_h+1} f_h \leq & |z_h|^{\sigma-\sigma_h+1} \left(\|W_h^*\| \, \|\Phi_h(Z_h)\| + \varepsilon_h^*\right) \\
\leq & \frac{1}{2d_h^2} z_h^{2(\sigma-\sigma_h+1)} \Theta_h^* \Phi_h^T(\chi_h) \Phi_h(\chi_h) + \frac{d_h^2}{2} + \frac{1}{2} z_h^{2(\sigma-\sigma_h+1)} + \frac{(\varepsilon_h^*)^2}{2}.
\end{aligned} \tag{67}$$

Using (67) in (65), one has

$$\begin{aligned}
\dot{V}_h \leq & -\sum_{\kappa=1}^{h-1} \frac{\beta_\kappa \pi}{\varsigma T_d} z_\kappa^{(1+\varsigma/2)(\sigma-\sigma_\kappa+2)} - \sum_{\kappa=1}^{h-1} \frac{\bar{\beta}_\kappa \pi}{\varsigma T_d} z_\kappa^{(1-\varsigma/2)(\sigma-\sigma_\kappa+2)} \\
& - \sum_{\kappa=1}^{h-1} \frac{\mathfrak{e}+\tilde{\mathfrak{e}}}{\tau_\kappa} \tilde{\Theta}_\kappa^2 - \frac{1}{\tau_h} \tilde{\Theta}_h \dot{\hat{\Theta}}_h - \frac{g_0}{\delta_0} r_1^{+(1+\varsigma)/2} - \frac{\bar{g}_0}{\delta_0} r_1^{-(1-\varsigma)/2} \\
& + M_{h-1} + l_{h,1}^* + l_{h,2}^* + m_h(t_0, t) + \frac{d_h^2}{2} + \frac{(\epsilon_h^*)^2}{2} \\
& + z_h^{\sigma-\sigma_h+1} \left(u^{\sigma_h}(t) + \frac{1}{2d_h^2} z_h^{\sigma-\sigma_h+1} \Theta_h^* \Phi_h^T(\chi_h) \Phi_h(\chi_h)\right) \\
& + \frac{1}{\tau_h} \tilde{\Theta}_h \left[\tau_h \frac{1}{2d_h^2} z_h^{2(\sigma-\sigma_h+1)} \Phi_h^T(\chi_h) \Phi_h(\chi_h) - \dot{\hat{\Theta}}_h\right] \\
& + \left(1 - (\sigma - \sigma_1 + 2) \tanh^{\sigma-\sigma_1+2} \left(\frac{z_1}{\mu}\right)\right) \frac{x_2^2 \lambda(x_2)}{\delta_0}.
\end{aligned} \tag{68}$$

The real control u and the adaptive law $\hat{\Theta}_h$ are formulated as

$$u = -\left(\frac{1}{2d_h^2} z_h^{\sigma-\sigma_h+1} \hat{\Theta}_h \Phi_h^T(\chi_h)\Phi_h(\chi_h) + \Gamma_h z_h^{\sigma_h} \frac{\beta_h \pi}{\varsigma T_d} z_h^{(1+\varsigma/2)(\sigma+1)-(\sigma-\sigma_h+1)}\right)^{\frac{1}{\sigma_\iota}}, \tag{69}$$

$$\dot{\hat{\Theta}}_h = \tau_h \frac{1}{2d_h^2} z_h^{2(\sigma-\sigma_h+1)} \Phi_h^T(\chi_h)\Phi_h(\chi_h) - 2(\mathfrak{e}+\tilde{\mathfrak{e}})\hat{\Theta}_h, \tag{70}$$

where $\beta_h = \frac{(3n)^{\frac{\varsigma}{2}}}{(\sigma-\sigma_\iota+2)(1+\varsigma/2)}$, $\bar{\beta}_h = \frac{1}{(\sigma-\sigma_h+2)^{(1-\varsigma/2)}}$, $\Gamma_h = \frac{\bar{\beta}_h \pi}{\varsigma T_d} + 1$, and $\hat{\Theta}_h(0) \geq 0$.

Using (69) in (70), one has

$$\begin{aligned}
\dot{V}_h \leq & -\sum_{\kappa=1}^{h-1} \frac{\beta_\kappa \pi}{\varsigma T_d} z_\kappa^{(1+\varsigma/2)(\sigma-\sigma_\kappa+2)} - \sum_{\kappa=1}^{h-1} \frac{\bar{\beta}_\kappa \pi}{\varsigma T_d} z_\kappa^{(1-\varsigma/2)(\sigma-\sigma_\kappa+2)} - \sum_{\kappa=1}^{h} \frac{\mathfrak{e}+\tilde{\mathfrak{e}}}{\tau_\kappa} \tilde{\Theta}_\kappa^2 \\
& - \Gamma_h z_h^{\sigma+1} - \frac{\beta_h \pi}{\varsigma T_d} z_h^{(1+\varsigma/2)(\sigma+1)} - \frac{\bar{\beta}_h \pi}{\varsigma T_d} z_h^{(1-\varsigma/2)(\sigma+1)} \\
& + \frac{\mathfrak{e}+\tilde{\mathfrak{e}}}{\tau_h} \Theta_h^{*2} - \frac{g_0}{\delta_0} r_1^{(1+\varsigma/2)} - \frac{\bar{g}_0}{\delta_0} r_1^{(1-\varsigma/2)} + \frac{\beta_h \pi}{\varsigma T_d} z_h^{(1-\varsigma/2)(\sigma+1)} + m_h(t_0,t) \\
& + \left(1 - (\sigma-\sigma_1+2)\tanh^{\sigma-\sigma_1+2}(z_1/\mu)\right) \frac{x_1^2 \lambda(x_1^2)}{\delta_0} + M_{h-1} + l_{h,1}^* + l_{h,2}^* + \frac{d_h^2}{2} + \frac{(\varepsilon_h^*)^2}{2}.
\end{aligned} \tag{71}$$

From Lemma 1, we have

$$z_h^{(1-\varsigma/2)(\sigma+1)} \leq \frac{\varsigma T_d \Gamma_h}{\bar{\beta}_h \pi} z_h^{\sigma+1} + \frac{\varsigma}{2}\left(\frac{\varsigma T_d \Gamma_h}{(1-\varpi/2)\bar{\beta}_h \pi}\right)^{1-2/\varsigma}. \tag{72}$$

Using (44), (45), and (72) in (71), one has

$$\begin{aligned}
\dot{V}_h \leq & -\sum_{\kappa=1}^{h-1} \frac{\beta_\kappa \pi}{\varsigma T_d} z_\kappa^{(1+\varsigma/2)(\sigma-\sigma_\kappa+2)} - \sum_{\kappa=1}^{h-1} \frac{\bar{\beta}_\kappa \pi}{\varsigma T_d} z_\kappa^{(1-\varsigma/2)(\sigma-\sigma_\kappa+2)} - \sum_{\kappa=1}^{h} \frac{\mathfrak{e}+\tilde{\mathfrak{e}}}{\tau_\kappa} \tilde{\Theta}_\kappa^2 \\
& - \frac{g_0}{\delta_0} r_1^{+(1+\varsigma)/2} - \frac{\bar{g}_0}{\delta_0} r_1^{-(1-\varsigma)/2} + M_h + \left(1 - (\sigma-\sigma_1+2)\tanh^{\sigma-\sigma_1+2}\left(\frac{z_1}{\mu}\right)\right) \frac{x_2^2 \lambda(x_2)}{\delta_0},
\end{aligned} \tag{73}$$

where

$$\begin{aligned}
M_h = m_h(t_0,t) + \frac{(\mathfrak{e}+\tilde{\mathfrak{e}})\Theta_h^{*2}}{2\tau_h} + \frac{\bar{\beta}_h \pi}{2T_d}\left(\frac{\varsigma T_d \bar{\Gamma}_h}{(1-\varsigma/2)\bar{\beta}_h \pi}\right)^{1-2/\varsigma} + \frac{(\beta_h+\bar{\beta}_h)\pi}{\varsigma T_d} \frac{\sigma_h - 1}{\sigma+1}\left[\frac{\sigma+1}{\sigma-\sigma_h+2}\right]^{-\frac{\sigma-\sigma_h+2}{\sigma_h-1}} \\
+ l_{h,1}^* + l_{h,2}^* + \frac{d_h^2}{2} + \frac{(\varepsilon_h^*)^2}{2} + M_{h-1}.
\end{aligned}$$

Consider the complete Lyapunov function as

$$V = \sum_{\kappa=1}^{h}\left(\frac{z_\kappa^{\sigma-\sigma_\kappa+2}}{\sigma-\sigma_\kappa+2}\right) + \sum_{\kappa=1}^{h}\left(\frac{1}{2\tau_\kappa}\tilde{\Theta}_\kappa^2\right) + \frac{r}{\delta_0}. \tag{74}$$

According to [38], there exists a positive constant Υ^* such that the parameter estimation error satisfies $\|\tilde{\Theta}_\iota\| \leq \Upsilon^*$. Invoking Lemma 1 and choosing $\mathcal{P} = \tilde{\Theta}_\iota$, $\epsilon = \aleph = 1$, $\tilde{c} = 2-\varsigma$, and $\tilde{d} = \varsigma$, one has

$$-\frac{2-\varsigma}{2}\tilde{\Theta}_\iota^2 \leq -(\tilde{\Theta}_\iota^2)^{1-\varsigma/2} + \frac{\varsigma}{2}, \tag{75}$$

$$-\frac{2-\varsigma}{2}\tilde{\Theta}_\iota^2 \leq -(\tilde{\Theta}_\iota^2)^{1+\varsigma/2} + \frac{\varsigma}{2}(\Upsilon^*)^4. \tag{76}$$

Based on the inequalities in [38], it follows that

$$-\sum_{\kappa=1}^{h}|x_\kappa|^{\check{L}} \le -\left(\sum_{\kappa=1}^{h}|x_\kappa|\right)^{\check{L}}, \quad 0<\check{L}\le 1, \tag{77}$$

$$-\sum_{\kappa=1}^{h}|x_\kappa|^{\check{L}} \le -h^{1-\check{L}}\left(\sum_{\kappa=1}^{h}|x_\kappa|\right)^{\check{L}}, \quad 1<\check{L}\le \infty, \tag{78}$$

where $x_\kappa \in \mathbb{R}$ for all $\kappa = 1, 2, \ldots, h$.

By employing (75)–(78) and differentiating V, one obtains

$$\begin{aligned}\dot{V} &\le -\frac{\pi}{\varsigma T_d}\left[\sum_{\kappa=1}^{h}\frac{z_\kappa^{\sigma-\sigma_\kappa+2}}{\sigma-\sigma_\kappa+2}+\sum_{\kappa=1}^{h}\frac{\tilde{\Theta}_\kappa^2}{2\tau_\kappa}+\frac{r}{\delta_0}\right]^{1+\varsigma/2}-\frac{\pi}{\varsigma T_d}\left[\sum_{\kappa=1}^{h}\frac{z_\kappa^{\sigma-\sigma_\kappa+2}}{\sigma-\sigma_\kappa+2}+\sum_{\kappa=1}^{h}\frac{\tilde{\Theta}_\kappa^2}{2\tau_\kappa}+\frac{r}{\delta_0}\right]^{1-\varsigma/2}\\ &\quad+\left(1-(\sigma-\sigma_1+2)\tanh^{\sigma-\sigma_1+2}(z_1/\mu)\right)\frac{x_2^2\lambda(x_2)}{\delta_0}+\bar{B}_h\\ &\le -\pi\omega_d^T V^{1+\omega/2}-\pi\omega_d^T V^{1-\omega/2}+\left(1-(\sigma-\sigma_1+2)\tanh^{\sigma-\sigma_1+2}(z_1/\mu)\right)\frac{x_2^2\lambda(x_2)}{\delta_0}+B_h,\end{aligned} \tag{79}$$

where $\bar{B}_h = \frac{h(3n)^{\varsigma/2}\pi}{2^{2+\varsigma/2}\tau_h^{1+\varsigma/2}T_d}\Upsilon^{*4}+\frac{h\pi}{2^{2-\varsigma/2}\tau_h^{1-\varsigma/2}T_d}+B_h$.

Theorem 1. *For the nonlinear system described in (1), suppose that Assumptions 1–4 hold. When the control inputs are designed according to (36), (54), and (69) and the adaptive update mechanisms are selected as in (37), (55), and (69), it follows that every signal of the resulting closed-loop system remains bounded when starting from bounded initial states. Moreover, the tracking error is driven into a sufficiently small neighborhood of the origin within a user-prescribed finite time interval.*

Proof. From the Lyapunov-based analysis, it follows that the terms $-\frac{\pi}{\varsigma T_d}V^{1+\varsigma/2}$ and $-\frac{\pi}{\varsigma T_d}V^{1-\varsigma/2}$ are negative definite. Moreover, $\bar{B}_h$ is a bounded constant. The sign of the remaining term,

$$\left(1-(\sigma-\sigma_1+2)\tanh^{\sigma-\sigma_1+2}\left(\frac{z_1}{\mu}\right)\right)\frac{x_2^2\lambda(x_2)}{\delta_0},$$

is governed by the value of z_1. Accordingly, the analysis is divided into the following cases. □

Case 1. *Consider $z_1 \in \Omega_{z_1} = \{z_1 \mid |z_1| < 0.8814\,\mu\}$ for any $\mu > 0$. Since $z_1 = x_1 - y_r$, the boundedness of z_1 together with the bounded reference signal y_r guarantees that x_1 remains bounded. Furthermore, due to the smooth and non-negative nature of x_2^2, the term*

$$\left(1-(\sigma-\sigma_1+2)\tanh^{\sigma-\sigma_1+2}\left(\frac{z_1}{\mu}\right)\right)\frac{x_2^2\lambda(x_2)}{\delta_0}$$

is bounded. Let Ψ_0 denote its upper bound. Consequently, the time derivative of the Lyapunov function satisfies

$$\dot{V} \le -\frac{\pi}{\varsigma T_d}V^{1+\varsigma/2}-\frac{\pi}{\varsigma T_d}V^{1-\varsigma/2}+B^*, \tag{80}$$

where $B^* = \bar{B}_h + \Psi_0$.

Case 2. *$z_1 \notin \Omega_{z_1}$. By Lemma 4, we have $1-(\sigma-\sigma_1+2)\tanh^{\sigma-\sigma_1+2}\left(\frac{z_1}{\mu}\right) \le 0$.*

Thus, the Lyapunov derivative satisfies

$$\dot{V} \le -\frac{\pi}{\varsigma T_d}V^{1+\varsigma/2}-\frac{\pi}{\varsigma T_d}V^{1-\varsigma/2}+\bar{B}_h. \tag{81}$$

Combining both cases yields

$$\dot{V} \leq -\frac{\pi}{\varsigma T_d} V^{1+\varsigma/2} - \frac{\pi}{\varsigma T_d} V^{1-\varsigma/2} + B^*. \tag{82}$$

It follows from (82) that the time derivative of V satisfies the structural condition given in (24) of Lemma 8. As a consequence, the developed control scheme guarantees practical predefined-time stability of the tracking error for system (1). In particular, the Lyapunov function is ultimately bounded as $V < \frac{\varphi T_d B^*}{\pi}, \forall\, t > 2T_d$.

Figure 1 presents the block level illustration of the proposed control architecture, offering a clear overview of the overall control structure.

Remark 3. *The proposed predefined-time adaptive fuzzy control scheme involves algebraic control laws, first-order adaptive update equations, and evaluation of fuzzy basis functions. The online computational complexity mainly depends on the number of fuzzy rules employed in the approximation structure. Since no iterative optimization algorithms or matrix inversion operations are required, the controller implementation only involves standard arithmetic operations and differential equation updates. By selecting a moderate number of fuzzy rules, the computational burden remains manageable, making the proposed scheme suitable for real-time implementation on embedded processors and industrial control platforms.*

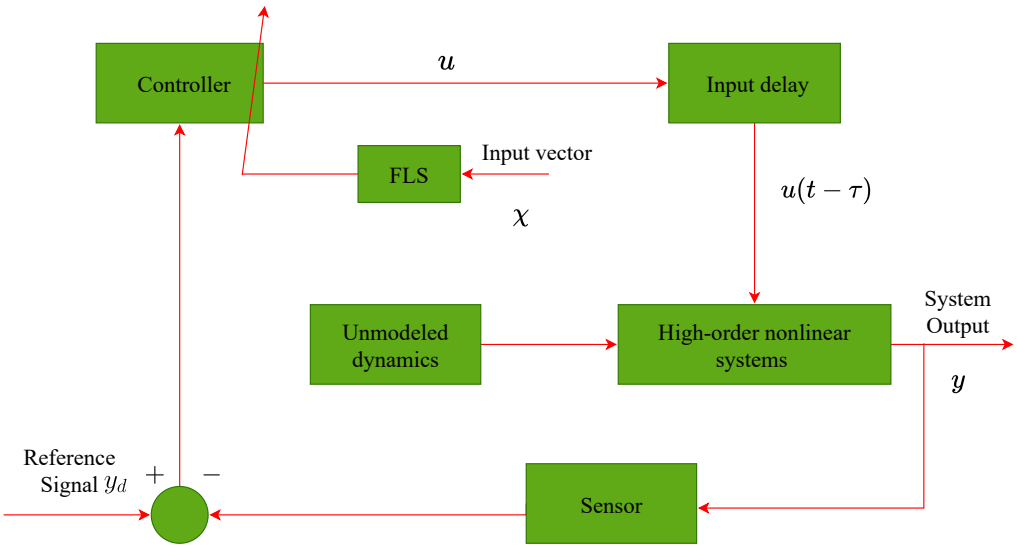

Figure 1. Block diagram depicting the structure of the developed control architecture.

Remark 4. *In this work, the input delay is assumed to be constant and sufficiently small relative to the dominant time constants of the closed-loop system. Here, a "small delay" refers to a delay magnitude for which the first-order Padé approximation provides an accurate low-order rational representation of the exponential delay term within the effective bandwidth of the system. It is acknowledged that this approximation introduces a bounded modeling error between the actual delayed signal and its rational approximation. Such residual error can be regarded as a lumped uncertainty, and may slightly influence transient performance. However, the boundedness of all closed-loop signals and the predefined-time practical stability property remain preserved under the proposed adaptive fuzzy framework provided that the delay satisfies the stated assumption.*

Remark 5. *In this work, the controller parameters are selected using a trial-and-error tuning procedure while satisfying the theoretical conditions derived from the Lyapunov stability analysis. The predefined-time parameter is chosen according to the desired convergence horizon, and the adaptive gains are adjusted iteratively to achieve a suitable tradeoff between convergence speed,*

steady-state accuracy, and control smoothness. It is observed that moderate variations in the design parameters mainly influence transient performance, whereas the boundedness of all closed-loop signals and the predefined-time practical stability property remain preserved provided that the stability conditions are maintained.

Remark 6. *Although the proposed control framework is developed from a theoretical perspective, it is motivated by practical engineering applications in which high-order nonlinear dynamics, input delays, and unmodeled uncertainties coexist. Typical application scenarios include aerospace attitude control systems, robotic manipulators, multi-agent coordination networks, and networked control systems with communication delays. From an implementation standpoint, the proposed predefined-time adaptive fuzzy controller mainly consists of algebraic computations, adaptive update laws, and fuzzy basis function evaluations, which can be executed in real time on embedded processors or industrial control platforms. The computational burden grows linearly with the number of fuzzy rules and system order, making the approach scalable for moderate-dimensional systems. Moreover, the predefined-time parameter allows for explicit adjustment of the convergence duration according to practical performance requirements, which enhances implementation flexibility.*

4. Simulation Results

This section provides two illustrative examples to verify the effectiveness of the proposed control approach and highlight its key characteristics.

Example 1. *Consider the high-order nonlinear system as*

$$\begin{cases} \dot{\xi} = -2\xi + 0.25x_1^2, \\ \dot{x}_1 = x_2^{\sigma_1} + x_2\cos(x_1^2) + \dfrac{\sin(x_1x_2)}{\sin^2(x_1)+1} + \Delta_1, \\ \dot{x}_2 = u^{\sigma_2}\big(t-\tau(t)\big) + x_1^2 + x_1x_2^2 + \Delta_2, \\ y = x_1, \end{cases} \tag{83}$$

where $f_1(x) = x_2\cos(x_1^2) + \dfrac{\sin(x_1x_2)}{\sin^2(x_1)+1}$, $f_2(x) = x_1^2 + x_1x_2^2$, $\Delta_1 = 0.5\xi^2x_1x_2$, $\Delta_2 = \xi^2\sin(x_1x_2)$, $\sigma_1 = 1$, $\sigma_2 = 2$ *and consequently* $\sigma = \max\{\sigma_1,\sigma_2\} = 3$. *Additionally, the input delay is modeled by* $\tau = 0.02$. *The reference trajectory is selected as* $y_d = \sin(0.5t)$. *The initial conditions are chosen as* $x_\iota(0) = 0.5$, $\hat{\Theta}_\iota(0) = 0$, *and* $r(0) = \xi(0)$, *for* $\iota = 1,2$. *The design constants are set to* $T_d = 2$, $\varsigma = 4/99$, $\tau_\iota = 0.5$, *and* $\delta_0 = 2$. *The fuzzy logic systems employ Gaussian-type basis functions given by* $\Phi_1 = \exp\Big[-\frac{(x_1-i)^2}{2}\Big]$ *and* $\Phi_2 = \exp\Big[-\frac{(x_1-i)^2}{2} - \frac{(x_2-j)^2}{2}\Big]$, *where the indices satisfy* $i,j,k \in \{-5,-4,\ldots,4,5\}$. *Define the nonlinear functions as* $\Psi_{1,1} = \frac{1}{4}x_1^2\sin^2(x_1)$, $\Psi_{2,1} = \frac{1}{4}x_1^2x_2^2$, *and* $\Psi_{1,2} = \Psi_{2,2} = \xi^2$. *Under these selections, Assumption 1 is satisfied. To fulfill Assumption 2, choose the Lyapunov candidate* $V(\xi) = \xi^2$ *together with* $\underline{\mathcal{L}}(\xi) = \frac{1}{2}\xi^2$ *and* $\bar{\mathcal{L}}(\xi) = \frac{3}{2}\xi^2$. *In accordance with Lemma 2, select* $\underline{g}_0 = \left(\frac{3}{\delta_0}\right)^{\varsigma/2}\frac{\pi}{\varsigma T_d}$, $\bar{g}_0 = \frac{j_0^{\frac{\varsigma}{2}}\pi}{\varsigma T_d}$, $\lambda(x_1^2) = \frac{5}{4}x_1^2$, $\bar{\omega} = \frac{14}{25}$. *Consequently, the auxiliary dynamic signal* r *evolves according to* $\dot{r} = -\underline{g}_0 r^{1+\varsigma/2} - \bar{g}_0 r^{1-\varsigma/2} + \frac{5}{4}x_1^4 + \frac{1}{25}$.

The first-step virtual controller α_1 *is synthesized following the design in (36), while the real control signal* u *is generated in accordance with (69). The parameter estimation dynamics* $\dot{\hat{\Theta}}_1$ *and* $\dot{\hat{\Theta}}_2$ *are specified by the update laws given in (55).*

The performance of the proposed adaptive control scheme is evaluated through the simulation results shown in Figures 2–7. Figure 2 compares the system output y with the desired reference signal y_r, from which it can be observed that the output accurately follows

the reference trajectory, demonstrating satisfactory tracking behavior. The corresponding tracking error z_1 is shown in Figure 3, where it is seen to gradually decrease and remain confined within a small region near the origin, indicating successful achievement of the tracking objective. Figure 4 illustrates the time response of the state variable x_2. The results indicate that x_2 stays within acceptable bounds throughout the simulation interval, which supports the stability of the closed-loop system. The evolution of the estimated parameters $\hat{\Theta}_1$ and $\hat{\Theta}_2$ is presented in Figure 5. Their bounded and well-behaved trajectories confirm the ability of the adaptive laws to compensate for parametric uncertainties. The control input u together with the delayed signal $u(t-\tau)$ is shown in Figure 6. Both signals vary smoothly over time, demonstrating that the input delay does not induce oscillations or destabilizing effects. Finally, Figure 7 depicts the unmodeled dynamics ξ and r, which remain bounded during the entire simulation. Overall, these simulation outcomes verify that the proposed control framework ensures the boundedness of all system signals while maintaining reliable and accurate tracking performance.

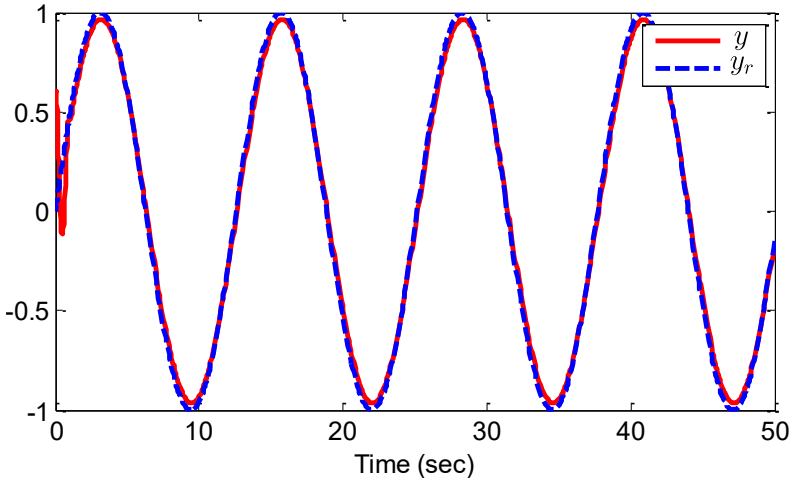

Figure 2. Trajectories of y and y_r.

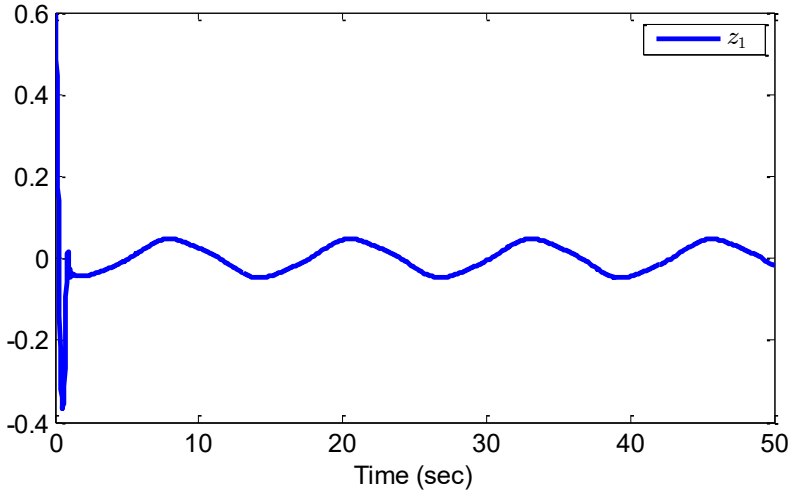

Figure 3. Trajectory of the tracking error z_1.

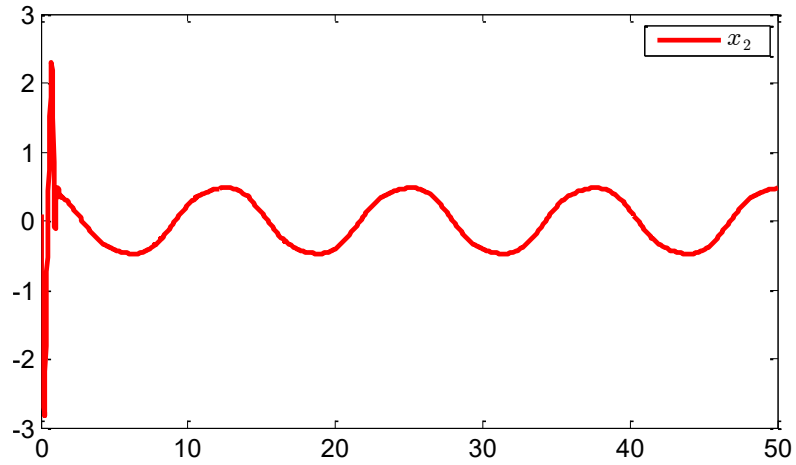

Figure 4. State variables x_2.

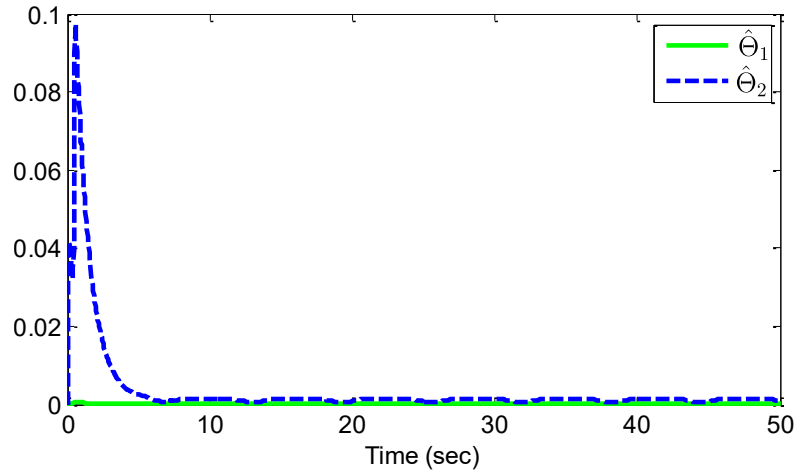

Figure 5. Adaptive laws $\hat{\Theta}_1$ and $\hat{\Theta}_2$.

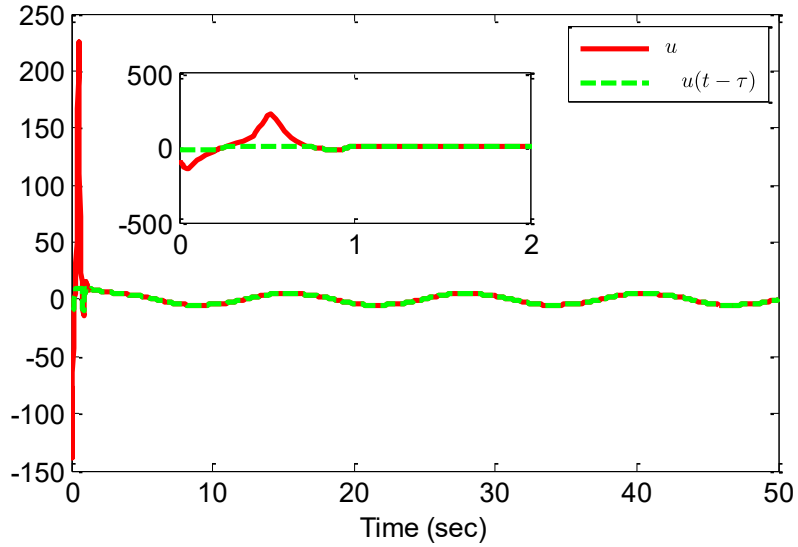

Figure 6. System input $u(t-\tau)$ and control input u.

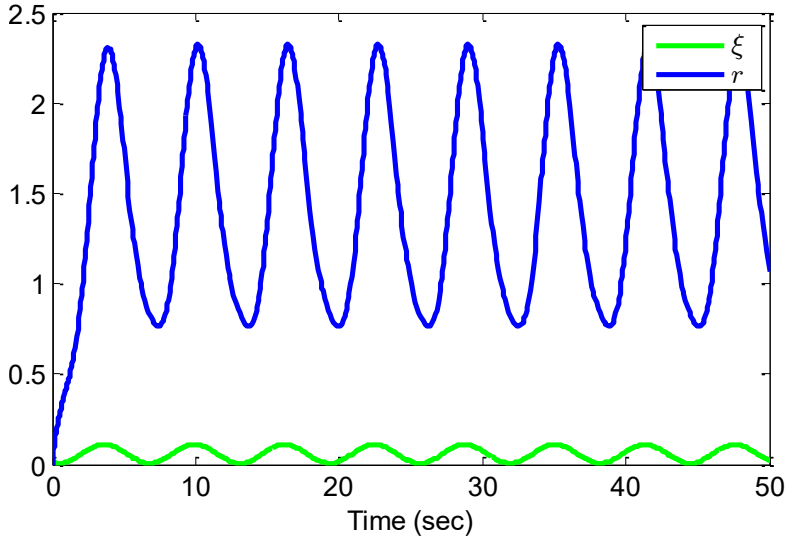

Figure 7. Trajectories of ξ and r.

Performance comparison using tracking error indices: To quantitatively assess the effectiveness of the proposed predefined-time adaptive fuzzy tracking controller, a comparative analysis is performed against representative fixed-time and finite-time control schemes [32,33] under identical simulation conditions. The comparison is performed for the considered nonlinear system subject to unmodeled dynamics and input time delay. Using N sampled data pairs $(y(t), y_r(t))$, several standard performance indices are adopted to assess tracking accuracy and convergence behavior.

Maximum absolute error (MAE):

$$\text{MAE} = \max_{1 \le t \le N} |y(t) - y_r(t)|. \tag{84}$$

Sum of squared error (SSE):

$$\text{SSE} = \sum_{t=1}^{N} (y(t) - y_r(t))^2. \tag{85}$$

Mean squared error (MSE):

$$\text{MSE} = \frac{1}{N} \sum_{t=1}^{N} (y(t) - y_r(t))^2. \tag{86}$$

Root mean squared error (RMSE):

$$\text{RMSE} = \sqrt{\frac{1}{N} \sum_{t=1}^{N} (y(t) - y_r(t))^2}. \tag{87}$$

Normalized mean squared error (NMSE):

$$\text{NMSE} = \frac{\sum_{t=1}^{N} (y(t) - y_r(t))^2}{\sum_{t=1}^{N} (y_r(t) - \bar{y}_r)^2}, \tag{88}$$

where $\bar{y}_d$ denotes the mean value of the desired trajectory.
{**Best** fit rate (BFR):}

$$C_{\mathrm{BFR}} = \left(1 - \frac{\sqrt{\sum_{t=1}^{N}(y(t) - y_r(t))^2}}{\sqrt{\sum_{t=1}^{N}(y_r(t) - \bar{y}_r)^2}}\right)100\%. \tag{89}$$

Table 1 presents the quantitative comparison results. It is observed that the proposed predefined-time adaptive fuzzy controller achieves the smallest MAE, SSE, MSE, and RMSE values, indicating superior transient and steady-state performance. The NMSE is significantly reduced while the BFR exceeds 99.6%, demonstrating highly accurate trajectory tracking. Compared with the fixed-time and finite-time methods [32,33], the proposed approach ensures faster convergence and tighter error bounds under identical operating conditions, validating the effectiveness of the predefined-time stability framework.

Table 1. Quantitative tracking performance comparison among predefined-time, fixed-time, and finite-time control schemes.

Method	MAE	SSE	MSE	RMSE	NMSE	BFR (%)
Proposed predefined-time scheme	0.018	0.00065	0.0000052	0.0023	0.0038	99.62
Fixed-time control scheme [33]	0.041	0.00360	0.0000288	0.0054	0.0175	98.32
Finite-time control scheme [32]	0.072	0.01140	0.0000912	0.0096	0.0520	94.80

Example 2. *Consider a practical application involving a one-link robotic manipulator with motor dynamics, as investigated in [50]. The dynamic equations of the system are given by*

$$\begin{cases} D\ddot{q} + B\dot{q} + N\sin(q) = I + I_d, \\ M\dot{I} + HI = -K_m\dot{q} + V, \end{cases} \tag{90}$$

where q, $\dot{q}$, and $\ddot{q}$ denote the link position, velocity, and acceleration, respectively. The variable I represents the generated motor torque, $I_d = \sin(\dot{q})\cos(I)$ denotes the disturbance torque, and V is the electromechanical control input. The system parameters are chosen as $D = 1\ \mathrm{kg}\cdot\mathrm{m}^2$, $B = 1\ \mathrm{N}\cdot\mathrm{m}\cdot\mathrm{s/rad}$, $N = 10\ \mathrm{N}\cdot\mathrm{m}$, $M = 0.3\ \mathrm{H}$, $H = 1.0\ \Omega$, and $K_m = 2\ \mathrm{N}\cdot\mathrm{m/A}$. It is assumed that the system is subject to input delay and unmodeled dynamics. Define the state variables as $x_1 = q$, $x_2 = \dot{q}$, $x_3 = I/D$, and the delayed control input as $u(t-\tau(t)) = \dfrac{V(t-\tau(t))}{DM}$.

Then, the system in (84) can be transformed as

$$\begin{cases} \dot{\xi} = -2\xi + 0.25x_1^2, \\ \dot{x}_1 = x_2^{\sigma_1} + \Delta_1, \\ \dot{x}_2 = x_3^{\sigma_2} - \dfrac{N}{D}\sin(x_1) - \dfrac{B}{D}x_2 + \dfrac{1}{D}\sin(x_2)\cos(Dx_3) + \Delta_2, \\ \dot{x}_3 = -\dfrac{K_m}{MD}x_2 - \dfrac{H}{MD}x_3 + u^{\sigma_2}(t-\tau(t)) + \Delta_3, \\ y = x_1, \end{cases} \tag{91}$$

where $f_1(x) = 0$, $f_2(x) = -\dfrac{N}{D}\sin(x_1) - \dfrac{B}{D}x_2 + \dfrac{1}{D}\sin(x_2)\cos(Dx_3)$, $f_3(x) = -\dfrac{K_m}{MD}x_2 - \dfrac{H}{MD}x_3$, $\Delta_1 = \xi x_1 x_2 x_3$, $\Delta_2 = \xi x_2\cos(x_1x_2)$, $\Delta_3 = \xi x_3\sin(x_1x_2)$, $\sigma_1 = 1$, $\sigma_2 = 1$, $\sigma_3 = 3$, and consequently $\sigma = \max\{\sigma_1, \sigma_2, \sigma_3\} = 3$. Additionally, the input delay is modeled by $\tau = 0.02$.

The reference trajectory is selected as $y_r = 0.5(\sin(t))$. The initial states and parameter estimates are chosen as $x_\iota(0) = 0.5$, $\hat{\Theta}_\iota(0) = 0$, and $r(0) = \xi(0) = 0$, for $\iota = 1, 2, 3$. The design constants are set to $T_d = 2$, $\varsigma = 4/99$, $\tau_\iota = 0.5$, and $\delta_0 = 2$.

The fuzzy logic systems employ Gaussian-type basis functions provided by $\Phi_1 = \exp\left[-\frac{(x_1-i)^2}{2}\right]$, $\Phi_2 = \exp\left[-\frac{(x_1-i)^2}{2} - \frac{(x_2-j)^2}{2}\right]$, $\Phi_3 = \exp\left[-\frac{(x_1-i)^2}{2} - \frac{(x_2-j)^2}{2} - \frac{(x_3-k)^2}{2}\right]$, where the indices satisfy $i, j, k \in \{-5, -4, \ldots, 4, 5\}$.

Define the nonlinear functions as $\Psi_{1,1} = \frac{1}{4}x_1^2 \sin^2(x_1)$, $\Psi_{2,1} = \frac{1}{4}x_1^2 x_2^2$, $\Psi_{3,1} = \frac{1}{4}x_3^2 \cos^2(x_1 x_2)$, and $\Psi_{1,2} = \Psi_{2,2} = \Psi_{3,2} = \xi^2$. Under these selections, Assumption 1 is satisfied; to fulfill Assumption 2, choose the Lyapunov candidate $V(\xi) = \xi^2$ together with $\underline{\mathcal{L}}(\xi) = \frac{1}{2}\xi^2$ and $\bar{\mathcal{L}}(\xi) = \frac{3}{2}\xi^2$. In accordance with Lemma 2, select $\underline{g}_0 = \left(\frac{3}{\delta_0}\right)^{\varsigma/2} \frac{\pi}{\varsigma T_d}$, $\bar{g}_0 = \frac{j_0^{\frac{\varsigma}{2}} \pi}{\varsigma T_d}$, $\lambda(x_1^2) = \frac{5}{4}x_1^2$, $\bar{\omega} = \frac{14}{25}$. Consequently, the auxiliary dynamic signal r evolves according to $\dot{r} = -\underline{g}_0 r^{1+\varsigma/2} - \bar{g}_0 r^{1-\varsigma/2} + \frac{5}{4}x_1^4 + \frac{1}{25}$.

The first-step virtual controllers α_1 and α_2 are synthesized following the design in (54), while the real control signal u is generated in accordance with (69). The parameter estimation dynamics $\dot{\hat{\Theta}}_1$, $\dot{\hat{\Theta}}_2$ and $\dot{\hat{\Theta}}_3$ are specified by the update laws given in (55). The performance of the proposed adaptive control method is evaluated through the simulation results depicted in Figures 8–13. Figure 8 presents the time responses of the system output y along with the desired reference signal y_r, showing close agreement and indicating that the controller achieves precise output tracking. The associated tracking error z_1 is shown in Figure 9, where it gradually decreases and remains within a small neighborhood of the origin, confirming the successful achievement of the tracking objective. The temporal behaviors of the state variables x_2 and x_3 are illustrated in Figure 10, demonstrating that both states remain bounded over the entire simulation period, which validates the stability of the closed-loop system under the proposed controller. Figure 11 depicts the evolution of the estimated adaptive parameters $\hat{\Theta}_1$, $\hat{\Theta}_2$, and $\hat{\Theta}_3$, with their bounded and smooth trajectories confirming the effectiveness of the adaptive laws in handling parametric uncertainties. Figure 12 compares the control input u with the delayed input $u(t-\tau)$; the smooth variations of these signals indicate that input delays do not introduce instability or undesirable oscillations. Finally, Figure 13 shows that the unmodeled dynamics ξ and r remain bounded throughout the simulation, further illustrating the robustness of the proposed approach. Collectively, these simulation results demonstrate that the developed control strategy ensures boundedness of all system signals while achieving accurate and reliable tracking performance.

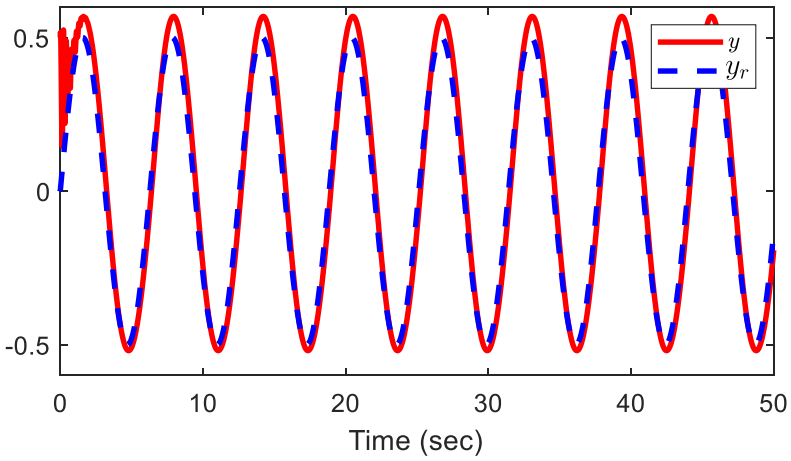

Figure 8. Trajectories of y and y_r.

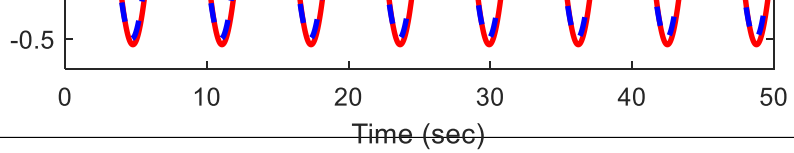

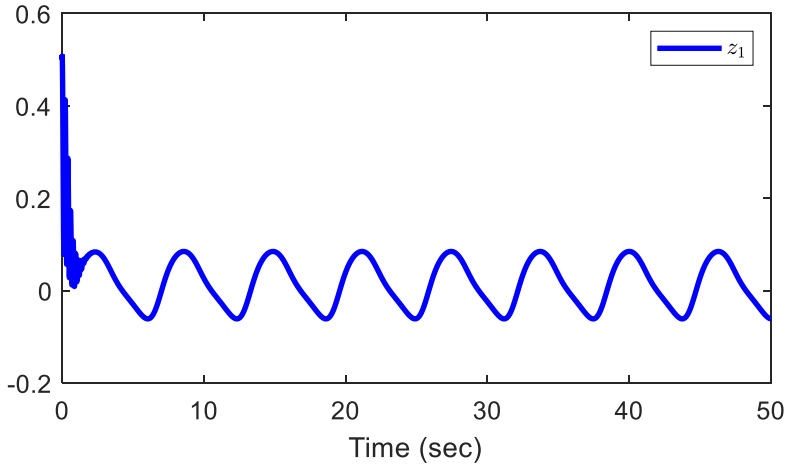

Figure 9. Trajectory of the tracking error z_1.

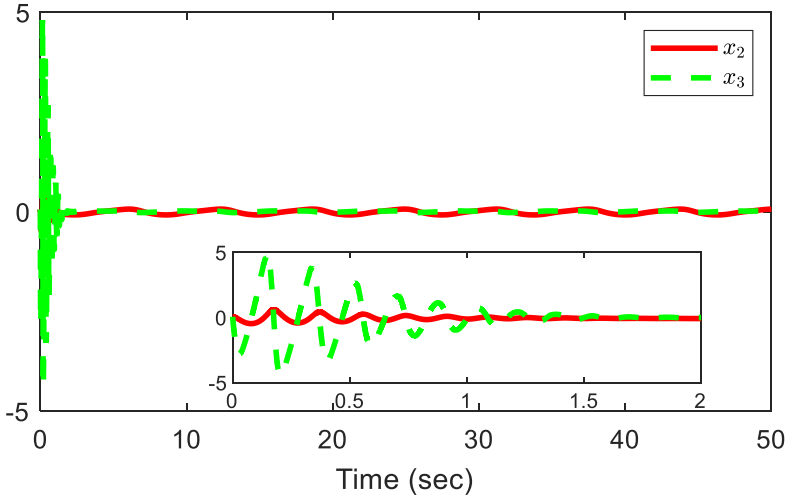

Figure 10. State variables x_2 and x_3.

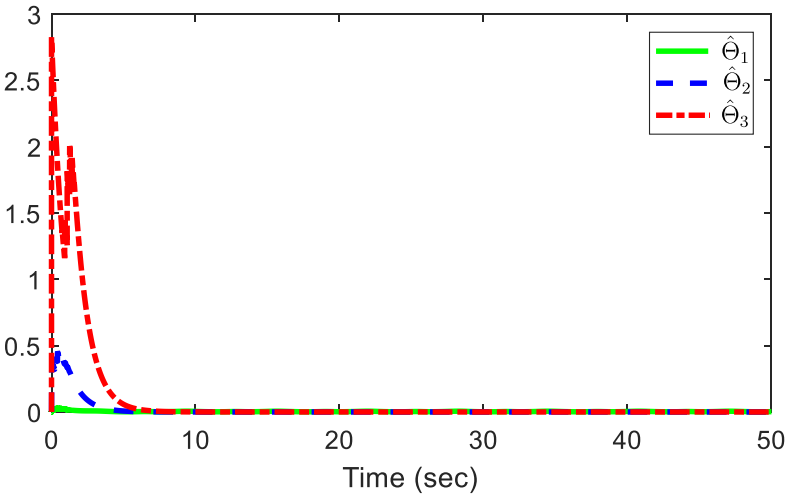

Figure 11. Adaptive laws $\hat{\Theta}_1$, $\hat{\Theta}_2$, and $\hat{\Theta}_3$.

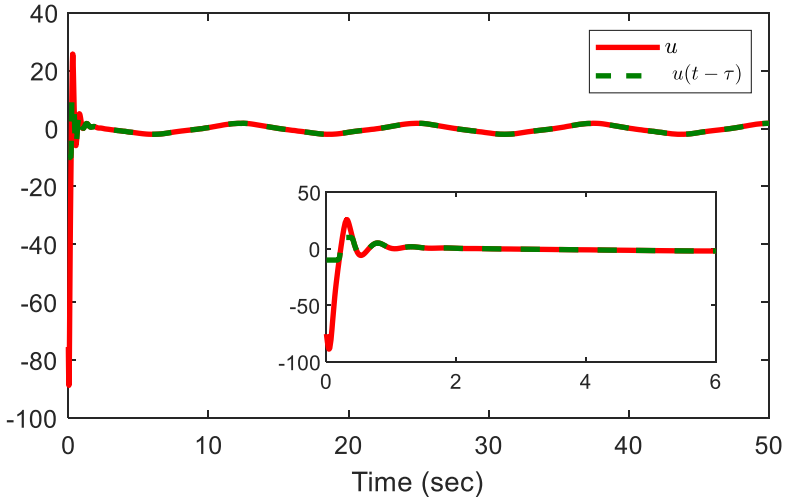

Figure 12. Control input u and system input $u(t-\tau)$.

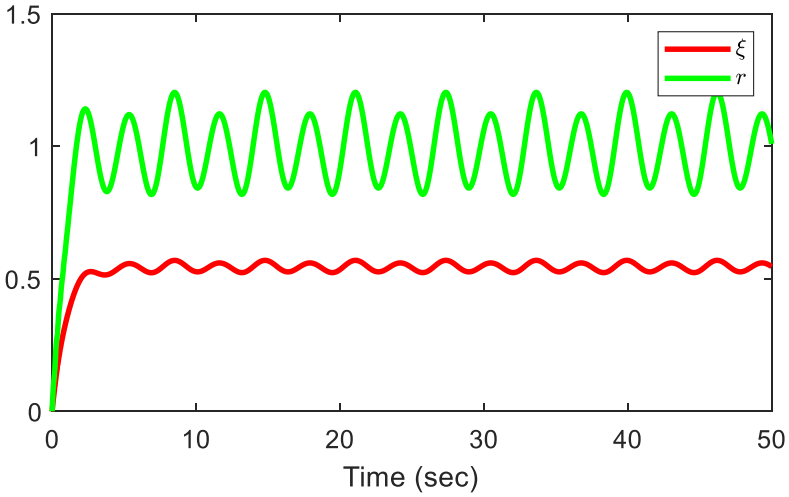

Figure 13. Trajectories of ξ and r.

Similar to Example 1, a comparative study is conducted under identical simulation conditions to quantitatively evaluate the effectiveness of the proposed predefined-time adaptive fuzzy tracking controller against representative fixed-time and finite-time control schemes [32,33].

Table 2 presents the quantitative tracking performance comparison for Example 2. It can be observed that the proposed predefined-time adaptive fuzzy controller achieves the smallest error indices among all compared methods. In particular, the MAE, RMSE, and NMSE values are significantly reduced while the BFR exceeds 99.7%, indicating highly accurate tracking performance. These results further confirm the superiority of the proposed scheme in terms of convergence precision and robustness.

Table 2. Tracking performance comparison for Example 2.

Method	MAE	SSE	MSE	RMSE	NMSE	BFR (%)
Proposed predefined-time scheme	0.015	0.00048	0.0000041	0.0020	0.0031	99.71
Fixed-time control scheme [33]	0.037	0.00310	0.0000260	0.0051	0.0158	98.54
Finite-time control scheme [32]	0.068	0.01020	0.0000850	0.0092	0.0476	95.24

5. Conclusions

This study has investigated the design of a predefined-time adaptive fuzzy control scheme for high-order nonlinear systems with nonstrict-feedback structures while considering the presence of unmodeled dynamics and input delays. A predefined-time auxiliary dynamic signal is incorporated to compensate for the effects of unmodeled dynamics, while the impact of input delays is alleviated using a Padé approximation in conjunction with an intermediate variable. Fuzzy logic systems are utilized to approximate the unknown nonlinear functions, reducing reliance on an accurate mathematical model of the system. By integrating the recursive backstepping technique with a power-type Lyapunov function framework, an adaptive fuzzy predefined-time tracking controller is developed. A comprehensive analytical study establishes that the designed feedback dynamics ensure practical predefined-time convergence of the closed-loop system, while suitable adjustment of the controller gains confines the tracking deviations within a small vicinity of the equilibrium point. The effectiveness and advantages of the proposed control strategy are further validated through simulation examples. Future research will focus on extending the proposed predefined-time adaptive fuzzy control framework to more complex nonlinear system classes. In particular, the extension to switched stochastic nonlinear systems will be investigated, where random disturbances, stochastic uncertainties, and switching behaviors coexist and significantly increase the difficulty of stability analysis and controller synthesis. Establishing predefined-time performance guarantees under stochastic effects and arbitrary switching signals while simultaneously addressing unmodeled dynamics and input delays remains an open and meaningful research direction. Moreover, robustness with respect to delay uncertainty and time-varying delays will be further explored to enhance the practical applicability of the approach. In addition, event-triggered control mechanisms and network-induced constraints will be incorporated in order to improve communication efficiency and reduce implementation burden in large-scale and distributed control systems.

Author Contributions: Conceptualization, M.K. and P.M.; Methodology, M.K. and P.M.; Software, M.K.; Validation, M.K. and P.M.; Formal analysis, M.K. and P.M.; Investigation, M.K. and P.M.; Resources, P.M.; Data curation, M.K. and P.M.; Writing—original draft, M.K.; Visualization, M.K.; Supervision, P.M.; Project administration, P.M.; Funding acquisition, P.M. All authors have read and agreed to the published version of the manuscript.

Funding: This research received no external funding.

Data Availability Statement: No data were used for the research described in the article.

Conflicts of Interest: The authors declare no conflicts of interest.

Abbreviations

Throughout this paper, $\mathbb{R}$ and $\mathbb{R}^n$ denote the sets of real numbers and n-dimensional real vectors, respectively. For the high-order nonlinear system given in (1), $x = [x_1, \ldots, x_h]^T \in \mathbb{R}^h$ represents the system state vector and $x_\iota = [x_1, \ldots, x_\iota]^T \in \mathbb{R}^\iota$ denotes the partial state vector for $\iota = 1, 2, \ldots, h$. The scalar output and control input are denoted by $y \in \mathbb{R}$ and $u \in \mathbb{R}$, respectively. The variable ξ represents the unmeasured internal state associated with unmodeled dynamics and $q(\cdot)$ describes the corresponding internal nonlinear dynamics. The functions $f_\iota(x), \iota = 1, \ldots, h$ denote unknown smooth nonlinear functions satisfying $f_\iota(0) = 0$, while $\Delta_\iota(x, \xi, t)$ represent unknown nonlinear disturbances. The constants $\sigma_\iota \geq 1$ are known odd integers. The term $\tau > 0$ denotes an unknown constant input delay. It is assumed that $q(\cdot)$ and $\Delta_\iota(\cdot)$ are locally Lipschitz-continuous. The notation $(\cdot)^T$ denotes matrix or vector transpose.

References

1. Zhang, Y.; Ning, X.; Wang, Z.; Yu, D. High-order disturbance observer-based neural adaptive control for space unmanned systems with stochastic and high-dynamic uncertainties. *IEEE Access* **2021**, *9*, 77028–77043. [CrossRef]
2. Kharrat, M.; Mercorelli, P. Neural network-based adaptive finite-time control for pure-feedback stochastic nonlinear systems with full state constraints, actuator faults, and backlash-like hysteresis. *Mathematics* **2025**, *14*, 30. [CrossRef]
3. Cui, Y.; Duan, G.; Liu, X.; Zheng, H. Adaptive fuzzy fault-tolerant control of high-order nonlinear systems: A fully actuated system approach. *Int. J. Fuzzy Syst.* **2023**, *25*, 1895–1906. [CrossRef]
4. Sui, S.; Chen, C.P.; Tong, S. Finite-time adaptive fuzzy prescribed performance control for high-order stochastic nonlinear systems. *IEEE Trans. Fuzzy Syst.* **2021**, *30*, 2227–2240. [CrossRef]
5. Deng, C.; Wen, C.; Wang, W.; Li, X.; Yue, D. Distributed adaptive tracking control for high-order nonlinear multiagent systems over event-triggered communication. *IEEE Trans. Autom. Control* **2022**, *68*, 1176–1183. [CrossRef]
6. Duan, G. High-order fully actuated system approaches: Part IV. Adaptive control and high-order backstepping. *Int. J. Syst. Sci.* **2021**, *52*, 972–989. [CrossRef]
7. Hou, M.; Shi, W.; Fang, L.; Duan, G. Adaptive dynamic surface control of high-order strict feedback nonlinear systems with parameter estimations. *Sci. China Inf. Sci.* **2023**, *66*, 159203. [CrossRef]
8. Liu, S.; Niu, B.; Zong, G.; Zhao, X.; Xu, N. Adaptive neural dynamic-memory event-triggered control of high-order random nonlinear systems with deferred output constraints. *IEEE Trans. Autom. Sci. Eng.* **2023**, *21*, 2779–2791. [CrossRef]
9. Niu, Y.; Yang, Y.; Wang, H.; Niu, B.; Shang, Z. Adaptive tracking control of high-order nonlinear systems with time-varying delays under asymmetric output constraints. *IEEE Trans. Autom. Sci. Eng.* **2024**, *22*, 2020–2030. [CrossRef]
10. Kharrat, M.; Mercorelli, P. Predefined-time adaptive command filter control for nonstrict-feedback nonlinear systems with input delay and unmodeled dynamics. *Mathematics* **2025**, *14*, 14. [CrossRef]
11. Shi, X.; Xu, S.; Jia, X.; Chu, Y.; Zhang, Z. Adaptive neural control of state-constrained MIMO nonlinear systems with unmodeled dynamics. *Nonlinear Dyn.* **2022**, *108*, 4005–4020. [CrossRef]
12. Wang, H.; Liu, P.X.; Li, S.; Wang, D. Adaptive neural output-feedback control for a class of nonlower triangular nonlinear systems with unmodeled dynamics. *IEEE Trans. Neural Netw. Learn. Syst.* **2017**, *29*, 3658–3668. [CrossRef]
13. Jiang, Z.P.; Praly, L. Design of robust adaptive controllers for nonlinear systems with dynamic uncertainties. *Automatica* **1998**, *34*, 825–840. [CrossRef]
14. Lyu, Z.; Liu, Z.; Xie, K.; Chen, C.P.; Zhang, Y. Adaptive fuzzy output-feedback control for switched nonlinear systems with stable and unstable unmodeled dynamics. *IEEE Trans. Fuzzy Syst.* **2019**, *28*, 1825–1839. [CrossRef]
15. Shen, Q.; Shi, P.; Wang, S.; Shi, Y. Fuzzy adaptive control of a class of nonlinear systems with unmodeled dynamics. *Int. J. Adapt. Control Signal Process.* **2019**, *33*, 712–730. [CrossRef]
16. Tong, S.; Li, Y. Adaptive fuzzy output feedback control for switched nonlinear systems with unmodeled dynamics. *IEEE Trans. Cybern.* **2016**, *47*, 295–305. [CrossRef]
17. Zhang, L.; Wang, P.; Hua, C. Adaptive control of time-delay nonlinear HOFA systems with unmodeled dynamics and unknown dead-zone input. *Int. J. Robust Nonlinear Control* **2023**, *33*, 2615–2628. [CrossRef]
18. Bi, W. Neural networks adaptive control for fractional-order nonlinear system with unmodeled dynamics and actuator faults. *IET Control Theory Appl.* **2023**, *17*, 259–269. [CrossRef]
19. Sui, S.; Chen, C.P.; Tong, S. Event-trigger-based finite-time fuzzy adaptive control for stochastic nonlinear system with unmodeled dynamics. *IEEE Trans. Fuzzy Syst.* **2020**, *29*, 1914–1926. [CrossRef]
20. Hua, Y.; Zhang, T. Adaptive control of pure-feedback nonlinear systems with full-state time-varying constraints and unmodeled dynamics. *Int. J. Adapt. Control Signal Process.* **2020**, *34*, 183–198. [CrossRef]
21. Li, D.P.; Liu, Y.J.; Tong, S.; Chen, C.P.; Li, D.J. Neural networks-based adaptive control for nonlinear state constrained systems with input delay. *IEEE Trans. Cybern.* **2018**, *49*, 1249–1258. [CrossRef]
22. Deng, W.; Yao, J.; Ma, D. Adaptive control of input delayed uncertain nonlinear systems with time-varying output constraints. *IEEE Access* **2017**, *5*, 15271–15282. [CrossRef]
23. Zhao, J.; Tong, S.; Li, Y. Observer-based fuzzy adaptive control for MIMO nonlinear systems with non-constant control gain and input delay. *IET Control Theory Appl.* **2021**, *15*, 1488–1505.
24. Wang, Y.; Zhang, J.; Zhang, H.; Xie, X. Adaptive fuzzy output-constrained control for nonlinear stochastic systems with input delay and unknown control coefficients. *IEEE Trans. Cybern.* **2020**, *51*, 5279–5290. [CrossRef]
25. Han, Y.Q. Design of decentralized adaptive control approach for large-scale nonlinear systems subjected to input delays under prescribed performance. *Nonlinear Dyn.* **2021**, *106*, 565–582. [CrossRef]
26. Li, Z.; Li, T.; Feng, G.; Zhao, R.; Shan, Q. Neural network-based adaptive control for pure-feedback stochastic nonlinear systems with time-varying delays and dead-zone input. *IEEE Trans. Syst. Man Cybern. Syst.* **2018**, *50*, 5317–5329. [CrossRef]
27. Qi, X.; Liu, W.; Lu, J. Observer-based finite-time adaptive prescribed performance control for nonlinear systems with input delay. *Int. J. Control Autom. Syst.* **2022**, *20*, 1428–1438. [CrossRef]

28. Han, Y.Q.; He, W.J.; Li, N.; Zhu, S.L. Adaptive tracking control of a class of nonlinear systems with input delay and dynamic uncertainties using multi-dimensional Taylor network. *Int. J. Control Autom. Syst.* **2021**, *19*, 4078–4089. [CrossRef]
29. Zhu, B.; Karimi, H.R.; Zhang, L.; Zhao, X. Neural network-based adaptive reinforcement learning for optimized backstepping tracking control of nonlinear systems with input delay. *Appl. Intell.* **2025**, *55*, 129. [CrossRef]
30. Zheng, X.Y. Adaptive neural control for non-strict feedback stochastic nonlinear systems with input delay. *Trans. Inst. Meas. Control* **2024**, *46*, 104–115. [CrossRef]
31. Kharrat, M. Finite-time fuzzy adaptive control for nonlinear systems with asymmetric dead-zone and actuator faults via an event-triggered mechanism. *Int. J. Adapt. Control Signal Process.* 2025, *in press*.
32. Kharrat, M. Neural network-based adaptive finite-time command-filter control for nonlinear systems with input delay and input saturation. *Int. J. Adapt. Control Signal Process.* **2025**, *39*, 231–243. [CrossRef]
33. Kharrat, M. Fixed-time adaptive tracking control for nonlinear systems with unmodeled dynamics and input dead-zone and saturation. *Int. J. Robust Nonlinear Control* 2025, *in press*.
34. Kharrat, M. Adaptive fixed-time command-filtered funnel control for nonstrict-feedback nonlinear systems with input saturation. *Trans. Inst. Meas. Control* 2025, *in press*. [CrossRef]
35. Kharrat, M.; Alhazmi, H. Fixed-time adaptive control for nonstrict-feedback nonlinear systems with sensor faults and input saturation. *J. Low Freq. Noise Vib. Act. Control* **2025**, *44*, 565–587. [CrossRef]
36. Kharrat, M.; Alhazmi, H. Fixed-time adaptive control for nonstrict-feedback nonlinear systems with input delay and unknown backlash-like hysteresis. *Neural Process. Lett.* **2025**, *57*, 52. [CrossRef]
37. Kharrat, M. Predefined-time adaptive fuzzy control for nonlinear cyber-physical systems under sensor and actuator attacks. *J. Vib. Control* 2025, *in press*. [CrossRef]
38. Zhao, L.; Sui, S.; Chen, C.P. Adaptive predefined-time control for high-order nonlinear systems with unmodeled dynamics. *Int. J. Adapt. Control Signal Process.* 2025, *in press*. [CrossRef]
39. Sui, S.; Chen, C.P.; Tong, S. Command filter-based predefined-time adaptive control for nonlinear systems. *IEEE Trans. Autom. Control* **2024**, *69*, 7863–7870. [CrossRef]
40. Wang, H.; Tong, M.; Zhao, X.; Niu, B.; Yang, M. Predefined-time adaptive neural tracking control of switched nonlinear systems. *IEEE Trans. Cybern.* **2022**, *53*, 6538–6548. [CrossRef]
41. Zhang, Y.; Chadli, M.; Xiang, Z. Predefined-time adaptive fuzzy control for a class of nonlinear systems with output hysteresis. *IEEE Trans. Fuzzy Syst.* **2022**, *31*, 2522–2531. [CrossRef]
42. Xu, H.; Yu, D.; Liu, Y.J. Observer-based fuzzy adaptive predefined-time control for uncertain nonlinear systems with full-state error constraints. *IEEE Trans. Fuzzy Syst.* **2023**, *32*, 1370–1382. [CrossRef]
43. Chen, P.; Tan, J.; Yao, Y.; Zhang, X.; Yao, Y. Predefined-time adaptive fuzzy control for nonlinear systems with input saturation and deferred restriction. *Nonlinear Dyn.* **2025**, *113*, 4727–4744. [CrossRef]
44. Yang, Y.; Sui, S.; Chen, C.P. Adaptive predefined-time control for stochastic switched nonlinear systems with full-state error constraints and input quantization. *IEEE Trans. Cybern.* 2025, *in press*.
45. Wang, L.; Xin, M.; Niu, J. Adaptive fuzzy predefined-time control for stochastic nonlinear systems against actuator and sensor faults. *IEEE Trans. Instrum. Meas.* 2025, *in press*.
46. Sui, S.; Zhao, L.; Chen, C.P. Adaptive fuzzy predefined-time tracking control design for nonstrict-feedback high-order nonlinear systems with input quantization. *IEEE Trans. Fuzzy Syst.* **2024**, *32*, 5978–5990. [CrossRef]
47. Ling, S.; Wang, H.; Liu, P.X. Adaptive tracking control of high-order nonlinear systems under asymmetric output constraint. *Automatica* **2020**, *122*, 109281. [CrossRef]
48. Cui, D.; Xiang, Z. Nonsingular fixed-time fault-tolerant fuzzy control for switched uncertain nonlinear systems. *IEEE Trans. Fuzzy Syst.* **2022**, *31*, 174–183. [CrossRef]
49. Wu, Y.; Xie, X.J.; Hou, Z.G. Adaptive fuzzy asymptotic tracking control of state-constrained high-order nonlinear time-delay systems and its applications. *IEEE Trans. Cybern.* **2020**, *52*, 1671–1680. [CrossRef] [PubMed]
50. Zhai, J.; Wang, H.; Tao, J.; He, Z. Observer-based adaptive fuzzy finite-time control for non-strict feedback nonlinear systems with unmodeled dynamics and input delay. *Nonlinear Dyn.* **2023**, *111*, 1417–1440. [CrossRef]